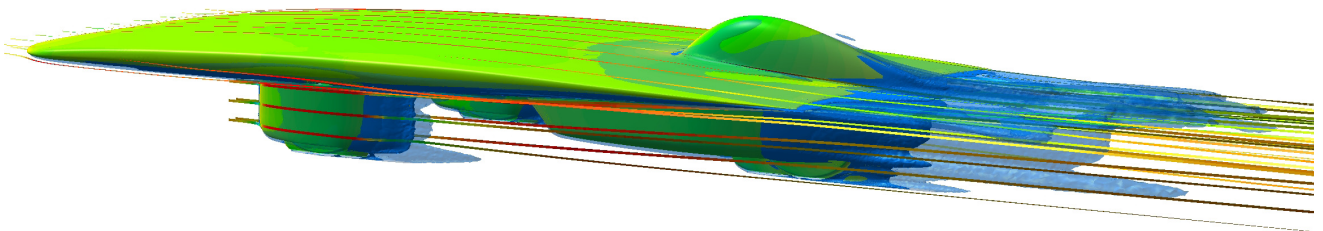


The Aerodynamic Design and Performance of Sunswift IV



By
Christopher Beves
Graham Doig

sunswift

Introduction



1.1 Introduction

Designing a car is not a simple task, if it were we would have all done it by now. Car companies spend several thousand hours and millions of dollars designing, manufacturing and testing each of their models. Literally hundreds of experienced engineers spend well over a year working on each new car, so why then should a ragged hand full of engineering students decide to undertake such a task?

Experience.

In the course of working on such a project, no matter if you a first year, a fourth year or even finished postgraduate there will be something to take away from starting with a blank piece of paper to rolling a car over the finish line many months later. Arguably you will probably learn more of what it means to be an engineer through doing this than you ever will getting HD's from first year to fourth year. Although experience is without doubt the primary goal, running a very close second is winning. With a racecar it has to be, from the outset we established IVy to be a solar powered racecar not simply a solar car.

This brings us to the actual core of the project, the World Solar Challenge (or the Global Green Challenge) from Darwin to Adelaide. It was required that a solar car of no more than 6m² of array and no wider than 1.8m be raced from start to finish. The challenge faced by the design is that it is light, low drag and have as highly efficient solar cells as affordable. In this case Silicon solar cells were all that could be used, thus putting reliance on drag optimisation. The goal was to create as low drag car in a range of operating conditions as possible, as the car has to drive in the real world not just in a wind tunnel. Therefore designing a shape that had the widest range of low drag stability was paramount, given that cross winds and gusts subject the car to more than just a direct head on flow with very low turbulence.

The design was going to be within a standard package based of other successful solar car packages, therefore none could go past NUNA. However several more steps were going to be taken to improve the design, plus give it a little more differentiation from other cars. It was to have performance and a little theatrics thrown in in order to give a car that can generate its own publicity and sponsorship. Letting the car do the talking speaks more to sponsors and people than anything else. However the most important thing in order to back this up with is *results*.

The “Bat-Wing” trailing edge

The first meeting resulted in two sketches that were practically identical, the three wheel layout with the canopy and bumpod hanging off the back of the car. The idea behind this was to promote the cleanest possible airflow over the main wing section by locating the two main sources of disturbance to the aerodynamics of the car as far downstream as possible, the canopy and the bumpod. Also incorporated was a waved trailing edge dubbed the bat-wing. The bat-wing trailing edge is to assist the air leaving the car, as with a straight trailing edge wing the air can leave equally at any point, which in an ideal wind tunnel works in theory, however in the real world it would be unstable and would oscillate. Thus by giving it a definite length to follow the flow would tend to stick to the car as long as possible, it would trail off at three defined hard points: the bumpod tail and the two wing tips. Additionally the tip extensions act similarly to winglets as you would see on a 747, minimising the very small vortices that would exist and reduce the turbulence and drag they cause, resulting in a wing with increased efficiency. On a 747 the large lift and stronger vortices generated by the ‘angle of attack’ the aircraft flies at necessitates they are quite pronounced vertically, whereas with IVy the low angle of attack results in lower forces and vortices thus the tip extension will alleviate these. It is very important in design to have a direction and the initial concept sketch is shown in figure 1.1.

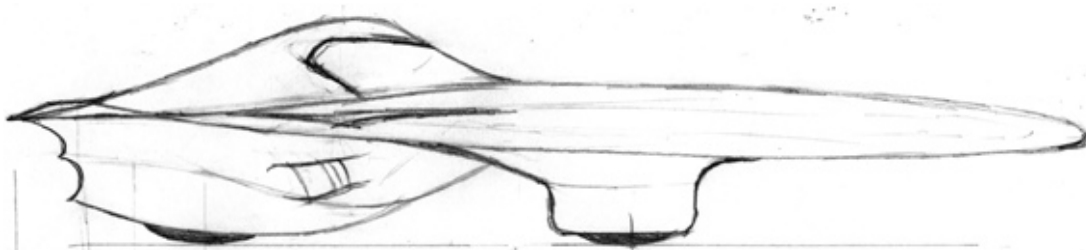


Figure 1.1 IVy Concept Sketch

The Challenges

The challenges faced relating to the initial design were seemingly many: a lack of existing design work on the car, lack of budget, lack of man power and a lack of time. These combined to limit the aerodynamic design and development phase to purely Computational Fluid Dynamics (CFD), which poses issues of its own which are addressed later. The lack of mechanical design posed the greatest challenge in that size had to be allowed for things that weren't even designed yet, such as the suspension size/travel limiting the thickness of the main wing as opposed to guessing based of previous cars with different weights/layouts. Ideally some preliminary work would have been already conducted. However, giving free reign to the aerodynamics allowed greater freedom, although a lot of additional work had to be thought through relating to driver ergonomics, suspension and the chassis.

Computational Fluid Dynamics

CFD is a tool and if you're not careful with it, it will make a tool out of you.

There are many text books on the subject, it has been a field that has been around for well over 35 years. Essentially it is using mathematical estimations of how fluids behave to simulate a problem numerically as opposed to studied experimentally. This is where the issue arises, people get used to how to use a software package and think what it tells them is correct, it is a computer after all isnt it? This assumption leads to sloppy results, the best way to view a pure CFD answer with no experimental data to check against it is with a healthy dose of scepticism. The problem is that its quite good at giving pretty pictures which are hard to argue with, and at the end of the day if they make a product brochure it makes for some great advertising and CFD's job is done. However when it comes to designing things purely in CFD alone there is a danger, there is no room for complacency and it is said often but hardly sinks in, however it is true of CFD: **GARBAGE IN = GARBAGE OUT.**

Ideally some wind tunnel work would have been conducted, so why even bother with CFD if apparently you cant design anything with it? You can, you just have to be very careful with it. CFD back in the day was really only supposed to be used to estimate the flow in a pipe, so designing a car with it is a big jump but not an impossible one. The big thing with the analysis is consistency and repeatability, which goes for both CFD and experimental measurement.

All that said, here is how to get at least a believable answer out of CFD.

The Mesh

Leaving the mathematics for the textbooks and lectures, it doesn't matter what turbulence model or to what order of accuracy you are solving for, if you don't have a decent mesh you will be purely doing CFD for the product brochure. It takes a while to understand what a good mesh is or how to even get one. However as a rule of thumb you want as many elements close to the surface as you can and as many elements as possible immediately downstream of the body to capture the wake (the flow that comes straight of the car), basically where the highest velocity gradients are and the most flow instability is expected to be. This will greatly increase the accuracy where it is needed, doubling the mesh in the middle of nowhere won't do anything. Figure 1.2 outlines this.

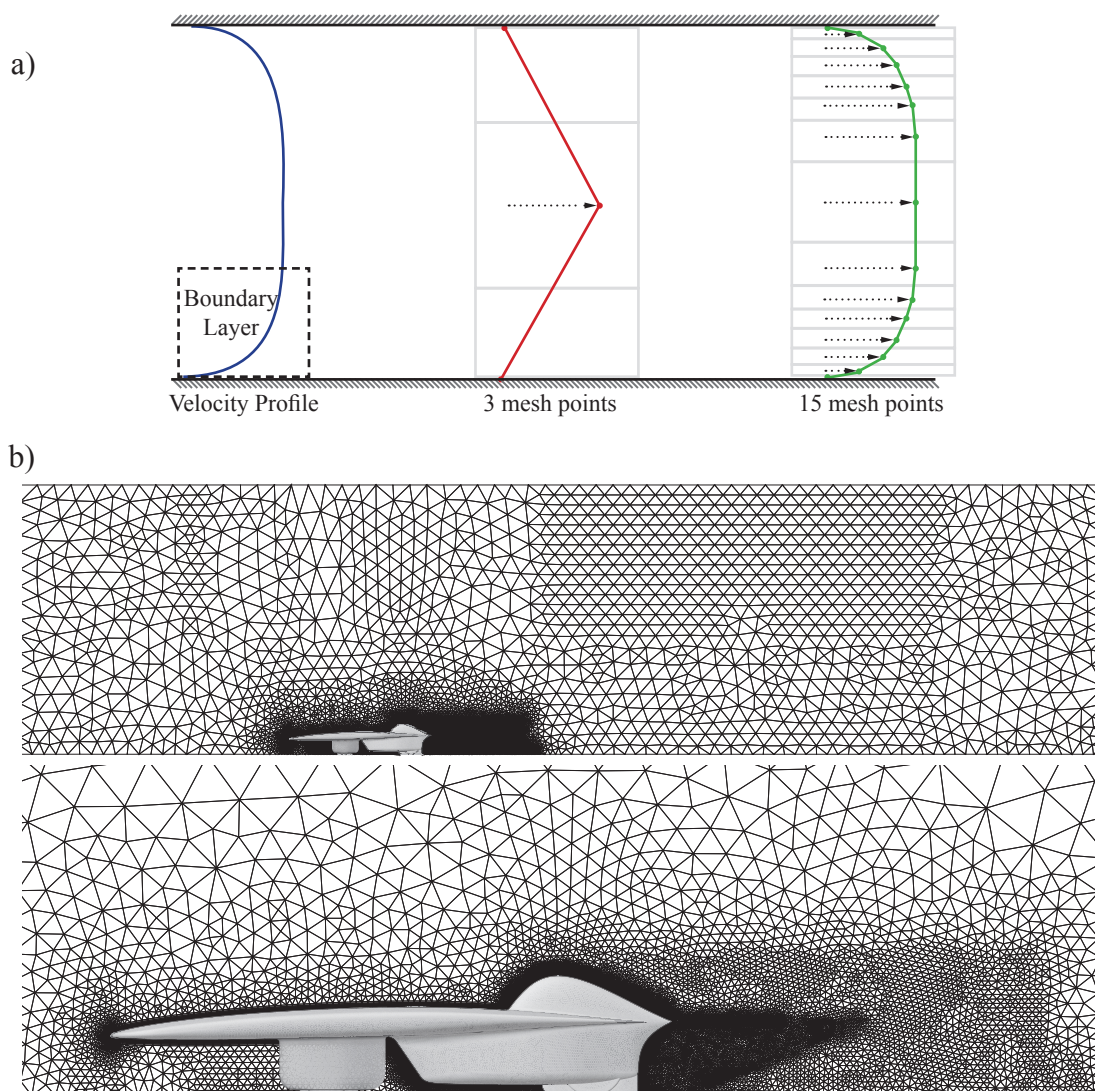


Figure 1.2 a) Actual Velocity profile (blue), under meshed (red), well meshed (green)
 b) Mesh around car

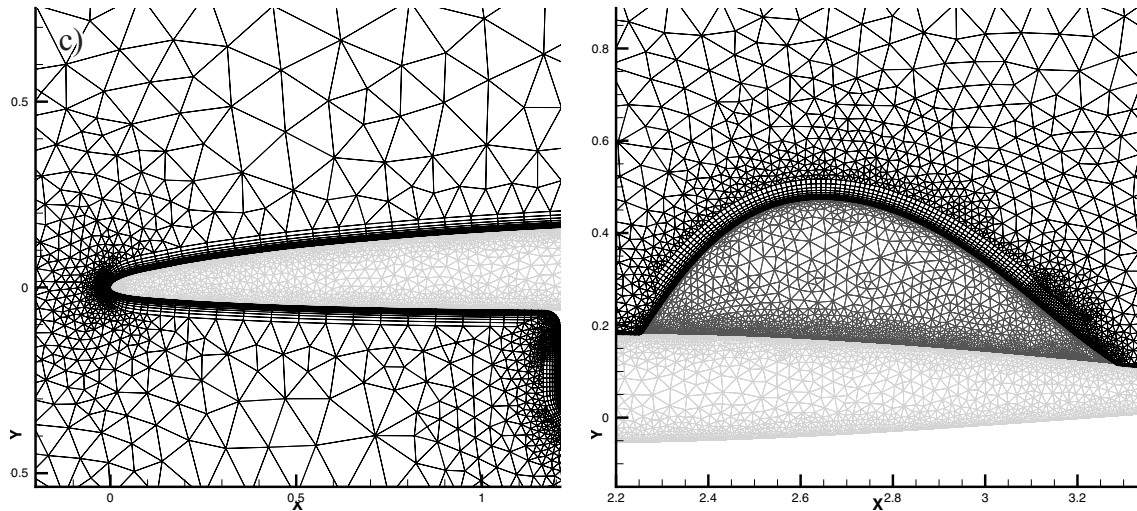


Figure 1.1 c) Leading Edge and Canopy Boundary Layer Mesh Detail

The Mesh Quality

It comes down to two things: squares or triangles. Having a mesh made up of primarily squares or three-dimensional cubes will give a more consistent, faster solution. The speed is increased as the number of elements in a mesh is a large factor in how long it takes to solve as 1 cube = 2 pyramids. The consistency and accuracy comes due to the fact that if a cell face is normal to a velocity vector there is less numerical error in calculating the velocity in the adjacent cell, figure 1.3 outlines this. In a high speed complex flow over a surface with various protrusions etc, the further down the body the flow gets, the more of these cells it has to move through the greater the error ends up being, and the higher the ‘skew’ or angle of the face the worse it gets.

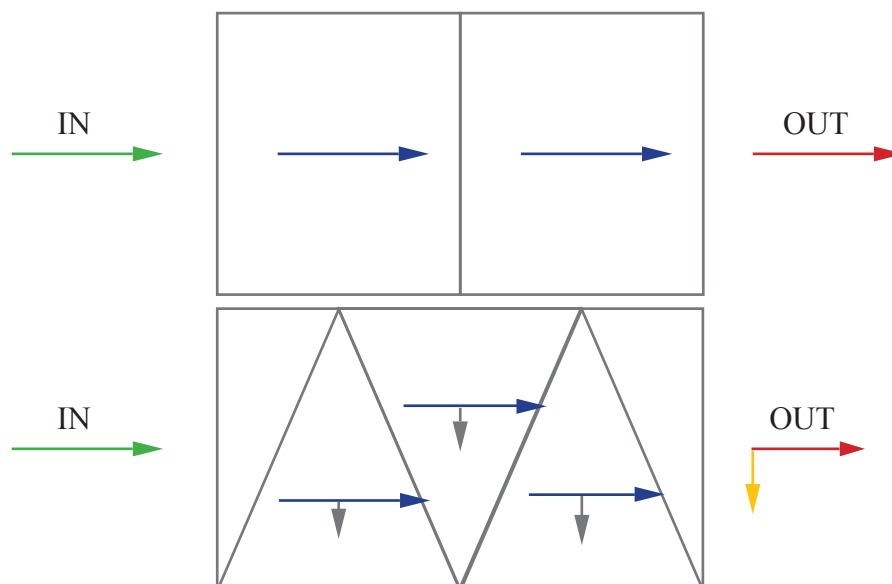


Figure 1.3 Mesh Quality and Associated Error or “false diffusion”

Now in figure 1.2 it may look like we have made the mistake of using the triangles in figure 1.3. Although on the surface of the car there are triangles in figure 1.2c, they are extruded normal to the surface, so the velocity tangent to the surface is still going through a mesh face that is more or less normal to it. So we have a situation where we are taking the best of both worlds as packing cubic elements around highly curved surfaces is time consuming given the software available to generate these meshes, yet at least keeping enough elements normal to the surface inside the boundary layer will minimise the problem shown in figure 1.3. If anything the mesh is maybe a little more packed with elements than it needs to be, but having tailored the number of elements in the mesh to the computing resources available we have struck enough of a balance between accuracy close to the surface and ease of mesh generation to push forward with confidence in the solution. Ideally studies would be conducted into how much finer it should be made and comparing the forces and pressures, there will be a point that no matter how fine you make the mesh, there is no more accuracy in the force result, known as a grid dependency check. Not having the time to conduct this, reliance was put on experience in meshing wings in ground effect to disregard this step and move forward .

Boundary Conditions

These are needed to tell the computer simulation what surface is what. In an aerodynamic CFD simulation there are 3 main types, a wall, an inlet and an outlet. A symmetry plane is occasionally needed for the cases where the flow is straight on to the car (i.e. no yaw) to half the number of mesh elements. The wall is set as 0 velocity for the car, as the flow next to the car is not moving. The wall representing the ground is set to the same speed as the inlet air velocity. If you consider a travelling car as a stationary object, the air and ground move over the car at the same speed by virtue of relative velocities. The inlet boundary condition specifies what velocity you wish to solve for and what level of turbulence you would expect. The outlet is basically a great big hole for the flow to leave the numerical model. The big issue that is faced is the correct placement of the boundary conditions. They cannot be too close to the body as it would affect the result, kind of like shoving a golf ball into a pipe and expecting the flow to be the same as a small rock. Figure 1.4 shows how far the boundaries are for the 0 yaw “symmetrical” case, obviously for the yawed cases

that simulate cross-wind the other half is added in. Walls are added on the top and side as well to stop flow leaking out and make a more stable solution. The placement of the inlet is 8m upstream of the car, the outlet is 20m downstream. The top and side walls are both 7m away from the car, the ground is set as per the designed car ground clearance. As with the grid dependency check mentioned earlier, a full check of the boundary condition location should also be conducted. Again with time as an issue a proper check was not carried out and experience was once again called on.

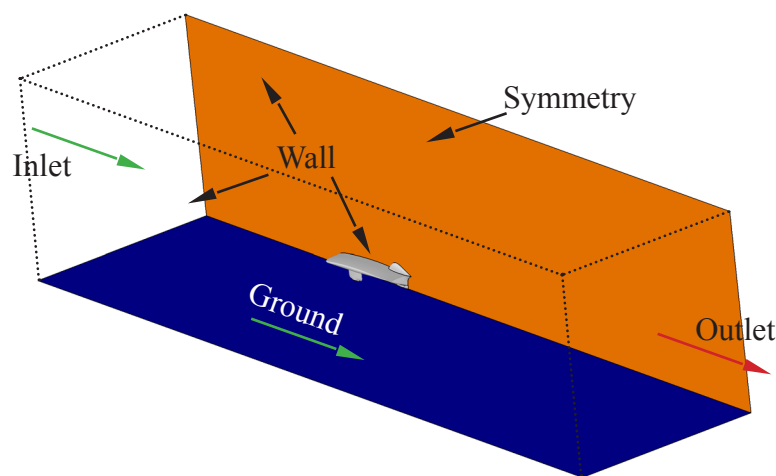


Figure 1.4 CFD Boundary Conditions for the no yaw case

Mesh Consistency

Comparing apples with apples makes it easier to pick up detail, comparing apples with oranges ends up with the answer of “well its small and round”, that level of accuracy doesn’t help at all with aerodynamic optimisation. When doing CFD on the car it was set that there should be no more than a 3% difference between the number of elements, otherwise the lift and drag would be impossible to correlate given that the forces can fluctuate quite rapidly with increased/decreased number of elements around the car; as in the grid dependency mentioned before. This was checked by both the number of elements on a surface of the car, and the total number in the whole mesh. The first dominates the force calculation (once the pressure is integrated over the surface) and the other dominates the accuracy of the flow field throughout the simulated ‘domain’.

Aerodynamic Terms

Ground Effect: If a body is in close proximity to the ground the flow between the ground and the body will accelerate causing a venturi effect. This will lead to increased lift or downforce given the correct shape, drag will also be influenced. At very low ground clearances drag will increase substantially.

Venturi Effect: A venturi duct reduces in cross sectional area, the reduced area leads to an increased velocity at the narrowest part of the duct which also reduces the pressure and is likely to be negative (suction).

Boundary Layer: The thin layer of fluid next to a surface (in figure 1.1a) where due to viscous forces the velocity increases from zero to the free stream speed.

Wake: The region of flow immediately coming off the body which is highly turbulent and has a low velocity as the fluid has been worked heavily by the shape.

C_D/C_L : Lift and drag or force coefficients that define the ability a shape has to generate the respective force component. It is a non-dimensional expression of the body forces to the shape (of the projected area component) and speed a body is travelling.

Aerodynamic Efficiency: A ratio of lift to drag to determine how efficient the lift is being generated, or how aerodynamically “neutral” an object is.

Pressure Coefficient “ C_p ”: The ratio of the static pressure deficit at a point (compared to the free stream) to the dynamic pressure. Typically $C_p=1$ at a stagnation point (where fluid initially hits a surface and is zero) and $C_p \ll 0$ where it is accelerated.

Turbulence: How chaotic and unstable a flow is.

Aero Map: A plot of lift, drag or side force for a given parameter (speed, yaw or ground clearance) to determine the aerodynamic characteristics of a body for car set-up or simulation purposes.

Moving Forward

Therefore in order to build up an idea of the basic layout we are after with the canopy and bumpod towards the rear of the car, a parametric study is carried out relating to the longitudinal position and shape of the canopy and bumpod. This is to determine how far back these can be placed without being detrimental to the performance of the car. The wheel faring position is also analysed before locking in the final shape. These are conducted with a basic configuration, but a final aeromap of a fully refined car is generated for both head on and yawed conditions at various car speeds.

Canopy Design

2

2.1 Introduction

The canopy design for IVy focused around the canopy placement along the length of the car, how long it should be and how much front curvature should exist (i.e., should it be flatter at the front or longer and pointed). The frontal area has to be large enough to accommodate a helmet (determining the width) and a legal roll hoop, determining the height. This is due to the height of the top of the canopy being governed by the rules relating to the driver position angle of 27° with some headroom and the minimum ground clearance required for the rear wheel to compress over a cattle grid/speed hump which was estimated to be approximately 80mm.

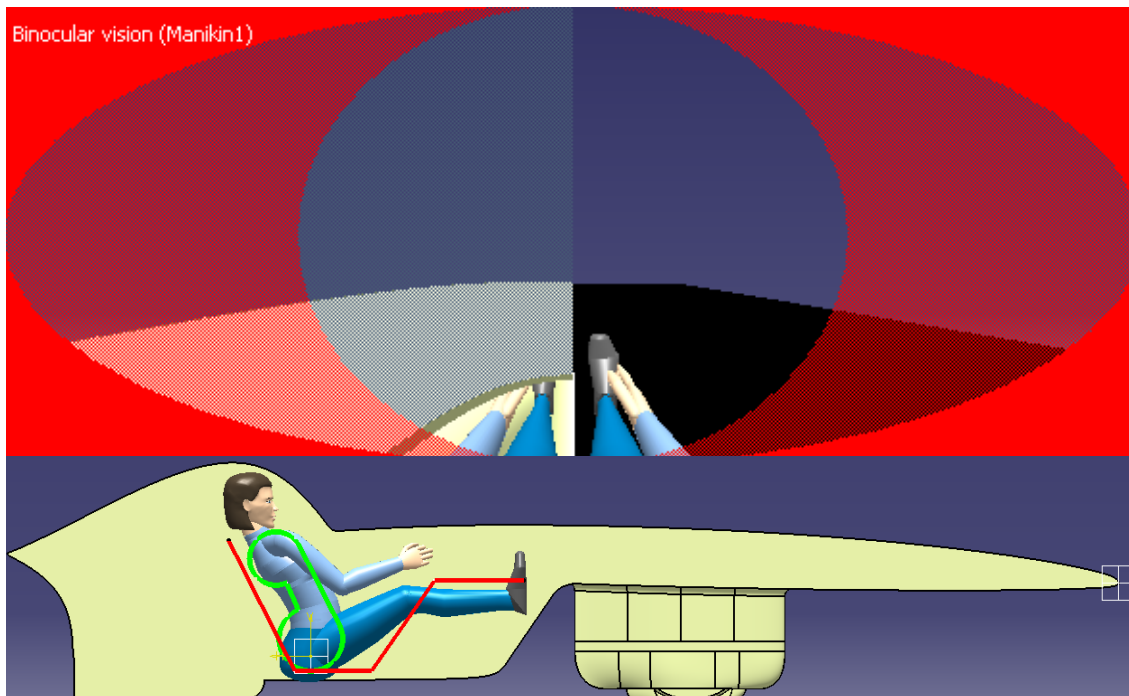


Figure 2.1 Driver Line of Sight, Mock up Canopy (red), 27° Seat Rule (green)

The main wing section was then “locked in” such that the driver’s shoulders were at least covered to satisfy the rule that the chassis rails form part of the driver

protection cell and the roll hoop does not have to be overly wide and triangular to encompass the shoulders. The rule stipulates if a sheet is covered over the front/rear roll hoops no part of the driver can breach that envelope. The main wing was placed as far away from the ground to minimize the “ground effect” interaction such a large wing would have (the drag more or less increases when a body gets very close to the ground), yet not so high the driver can’t see and the feet/pedal set could possibly be located in the main wing section. The CATIA manakin model of the driver in the car in figure 2.1 above indicates road visibility from 14.5m ahead on the road for the initial driver design position, however the final seating position in the car as it was made is different.

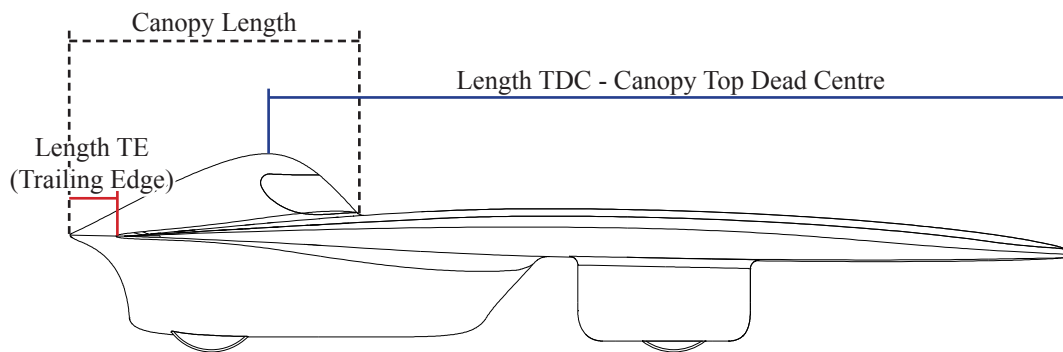


Figure 2.2 CFD Parameters for Canopy Design

The importance of the length-wise position of the canopy along the top shell may not be so obvious, some cars place them in the middle or towards the front perhaps purely due to layout or mechanical reasons; however for the best aerodynamics this may not be the case. It is possible that the disturbance the canopy creates to the flow over the top of the car can produce adverse air flow onto the main wing section (vortices can be generated which will increase drag). These effects can be increased greatly if there is a surface in contact with these flow interactions, so the net effect on drag for the whole car is greater than just adding on a carefully fully drag optimised canopy shape in a wind tunnel and placing it anywhere on the car. This is known as interference drag, as the name suggests it is because there is interference from another body. A good example is an aircraft; the net drag is higher than the sum of the drag for the individual fuselage/wings/engines/tail if they were measured

Table 2.1 CFD Parameter Values for Canopy Design

Length TDC	Length TE	Canopy Length	Speed 1	Speed 2
2650	30	1800	25	35
2650	30	2000	25	35
2900	300	1400	25	35
3150	50	1300	25	35
3150	50	1400	25	35
3150	50	1500	-	35

independently. This is a result of the underlying fluid mechanics and flow structures which a simplistic breakdown of aerodynamics into “frontal surface area” or “wetted area” fails to account for. For the case when the car is in a cross wind or a dynamic manoeuvre on a racetrack this too can be even more complicated. This prompted the need to get the main wing as far forward into un-disturbed flow and the bumpod and canopy as far back such that their wake (the lower velocity air left behind) was off the main wing and not interfering with any surface of the car, a layout that Nuna have used to good effect.

A simple model of the car was made with just the main wing, canopy and an exaggerated worst case bumpod (i.e. large). The parameters listed in table 2.1 do not reflect all the CFD cases solved or all of the cases that were wanted to be solved, but are the only ones that reliable answers were given for. Unfortunately there were continuing problems with the CFD as a result of several issues with the AC3 cluster that have been experienced before in other projects. Never the less whist it is a small data set the main trends were able to be established. This involved eliminating a few outliers in that whist the shape of the canopy in the rearward positions is extreme (little taper i.e., more “bubble like”), the forward cases were more ideal (longer and more streamlined). CFD accuracy between cases can be $\pm 2-5\%$ based on the quality of the mesh and the number of points in the mesh. Looking for a small improvement in drag (which CFD is O.K. but not great at predicting) is fraught with danger, especially without a wind tunnel to check against. The logic being that if the nicely shaped forward positioned canopy and the rearward placed ‘bad’ canopy give similar results for drag, then by improving the shape of the rearward canopy to be more streamlined, lower drag will result than the forward one, resulting in 2 cases to be solved instead of 6; not ideal but resources were limited.

2.2 Results

Looking at the velocity contours as in figures 2.3-2.8 shows three key aspects, low velocity at the very front of the canopy where the air flow hits the canopy and stops (a stagnation point), acceleration over the very top of the canopy and then a region of low velocity behind it (the wake). The differences are small, it may appear there is an improvement as there is less of a wake behind the canopy in figure 2.3 and figure 2.4, however the total wetted surface area is larger. Now that we are more or less comparing like-for-like in figures 2.3 and 2.4, and in figures 2.6, 2.7 and 2.8, a detail consideration like total wetted area will be of significance as it will influence the contribution the viscous effects place on the net drag component. The only meaningful way that we can compare the shapes is by looking qualitatively at the pressure distribution over the canopy surface as a direct result of how the air is accelerated and decelerated around over the surface and quantitatively at the resultant lift and drag forces. Additionally by virtue of the flow moving around the body, the disturbance to the flow will result in turbulence by the shape or some other flow feature (i.e, another body wake or vortex). A protrusion will locally increase turbulence as the flow around it becomes unsteady due to its presence; however it is essential that the shape itself does not generate large turbulent structures that penetrate significantly into the flow. In the case of the flow becoming fully turbulent around a body (i.e, separation), localised ‘jumps’ or changes in the pressure and turbulence distribution will occur.

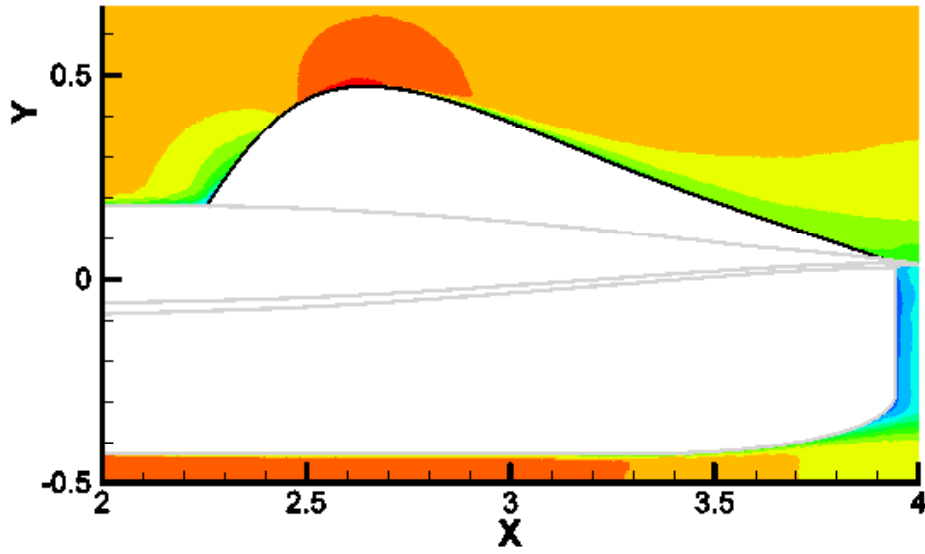


Figure 2.3 Canopy 2650-1800 (25 m/sec)

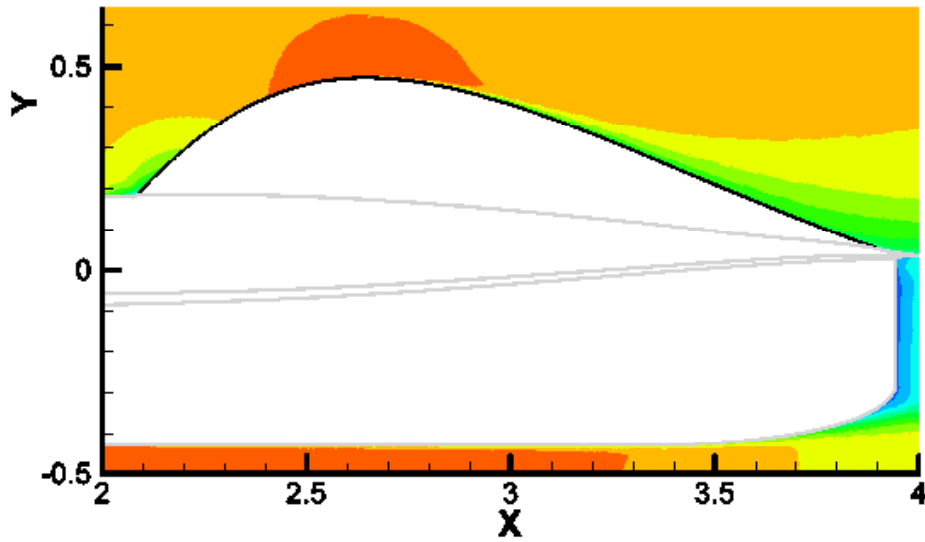


Figure 2.4 Canopy 2650-2000 (25 m/sec)

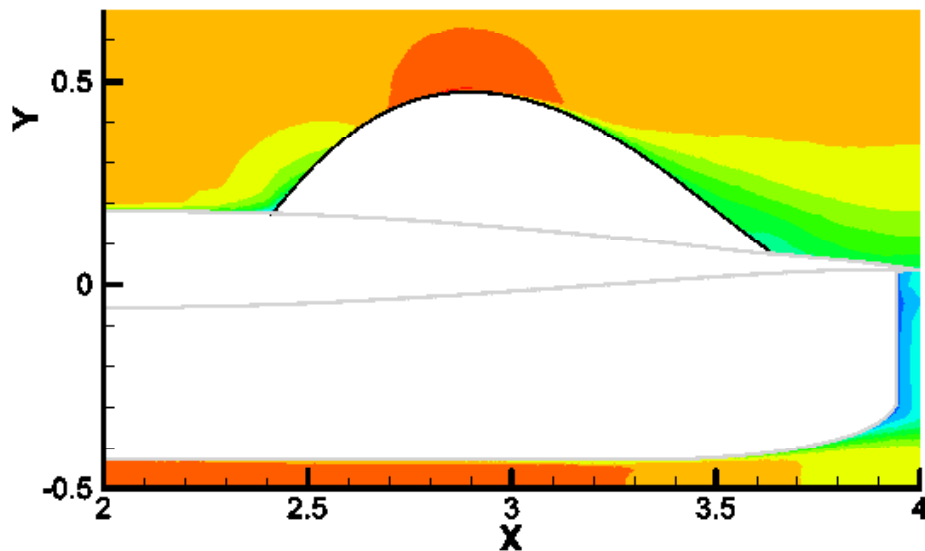


Figure 2.5 Canopy 2900-1400 (25 m/sec)

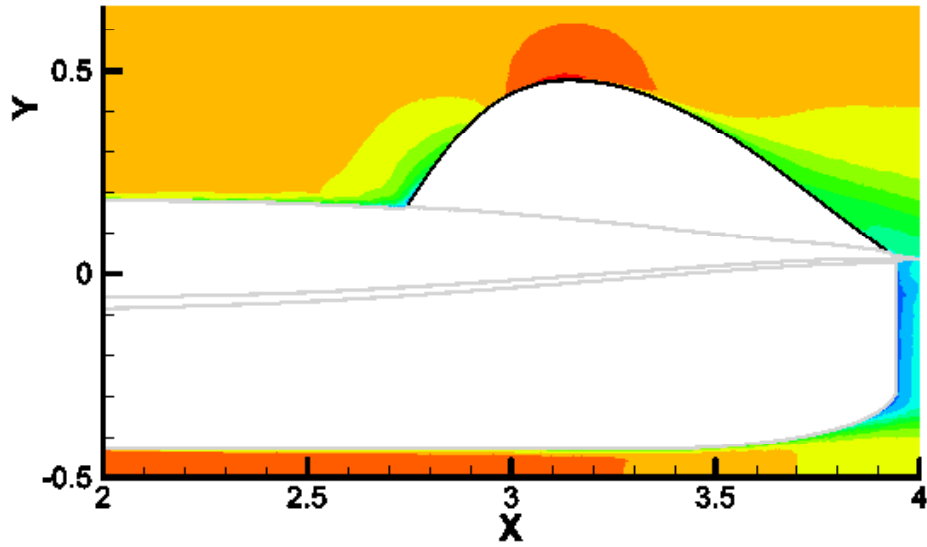


Figure 2.6 Canopy 3150-1300 (25 m/sec)

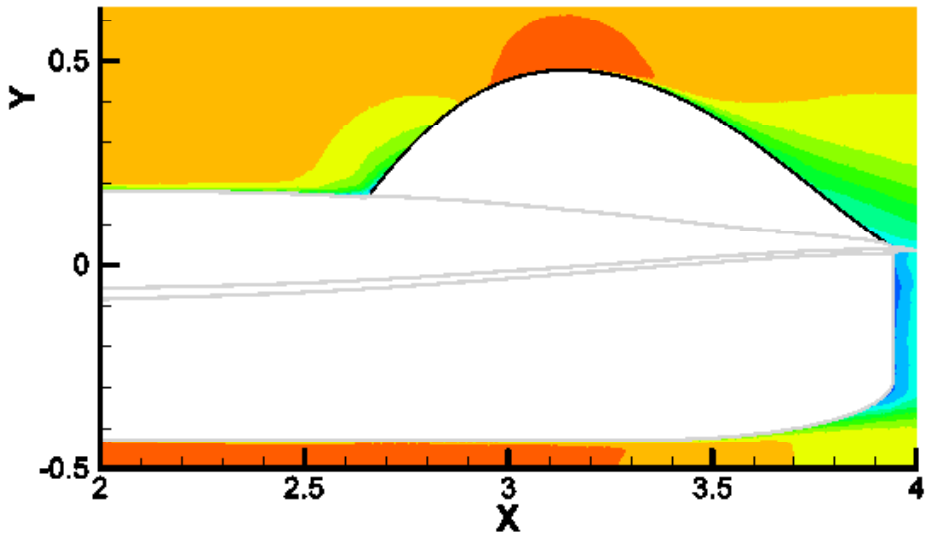


Figure 2.7 Canopy 3150-1400 (25 m/sec)

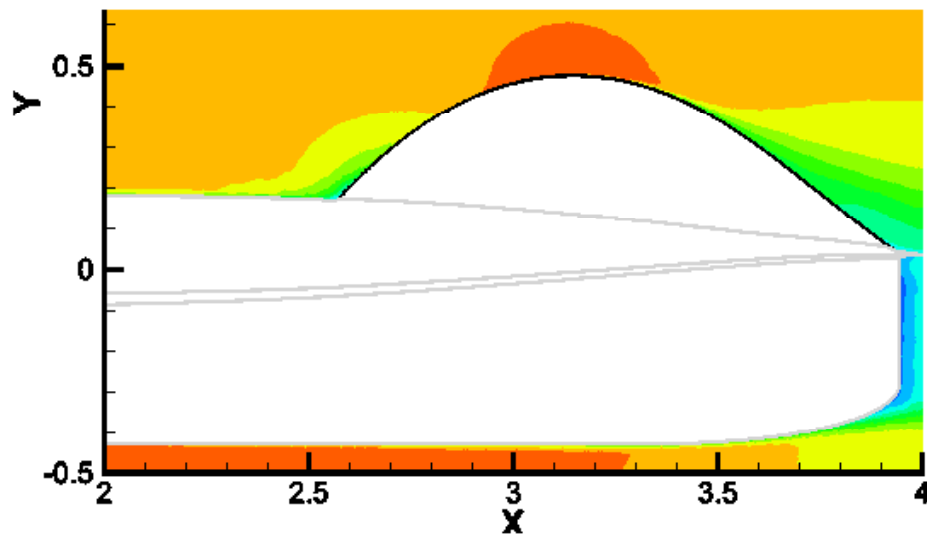


Figure 2.8 Canopy 3150-1500 (35 m/sec)

Force Report

Minimising both lift and drag from the canopy is important, table 2.2 outlines the lift and drag forces for the various canopy designs for the whole car, the ratio of lift to drag (aerodynamic efficiency) is also indicated. Minimising the lift will not only help in stability of the car, but it will also reduce the lift induced drag by virtue of the fact that lift never acts parallel to the vertical axis of a body, there is always some angle that splits it into x, y, z components.

Table 2.2 Canopy Design Lift, Drag and Aerodynamic Efficiency Values

Speed	25 m/s	25 m/s	Efficiency	35 m/s	35 m/s	Efficiency
Case	Drag (N)	Lift (N)	L/D	Drag (N)	Lift (N)	L/D
2650-1800	14.039	14.601	1.04	25.617	27.798	1.09
2650-2000	14.040	14.358	1.02	25.452	31.393	1.23
2900-1400	14.163	15.189	1.07	25.864	28.911	1.13
3150-1300	14.174	10.754	0.759	25.848	20.002	0.774
3150-1300	14.071	10.246	0.728	25.761	19.077	0.741
3150-1400	-	-	-	25.647	18.584	0.724

For the Drag values in table 2.2 at 25 m/sec it seems the drag is consistently 14N, and around 25.5N at 35 m/sec. It is important to note that although the drag values are similar, the shape and position of the canopy is not. The drag for the canopy placed at 3150mm with a less than ideal shape is similar to the canopy placed at 2650mm which is more slender and ideal. Upon checking what happens to the 1400mm length canopy (highlighted in red in table 2.2) when it is moved forward by 250mm to 2900mm the drag increases 0.1N (see also figure 2.5 and 2.7). Thus showing that the further forward the identically shaped canopy is placed the more drag there is, there is also an increase in lift by 5N to 15N (50%). So the further rearward the canopy is placed the better in minimising drag and lift. The data at 35 m/sec is a little more complete for the length increasing from 1300mm to 1400mm and 1500mm, which shows a drop in lift and drag as the amount of front canopy curvature is reduced. Thereby shifting the more ideally shaped canopy further towards the rear will reduce lift and drag due to the fact that the canopy is no longer positioned near the peak suction pressure of the top surface of the main wing and the oncoming air flow is not hitting the canopy as directly. This is noticeable in figure 2.6-2.8 by a smaller region of high velocity than figures 2.3-2.5 as the air accelerates less over the canopy bump.

Pressure Coefficient

Three things are evident when looking at the pressure coefficient contours in figures 2.9 to 2.13:

- 1) The high pressure at the front of the canopy (stagnation point) where the oncoming air hits it and is stationary, it can't move either side as it is essentially trapped by air moving either side of the canopy.
- 2) The thickest part of the canopy, where the airflow accelerates the most around the curvature of the canopy shape causing low pressure
- 3) How much the lines are bunched up or spread out depending on the shape.

The high pressure at the front seems to alter with the length of the canopy changing at a given canopy position (compare figures 2.9 to 2.10). As the front curvature is flatter, the flow has more time to 'react' to the shape and acts over a larger area. This will then require a better shape behind it to slowly assist the pressure to recover (gradually increase again). The shorter canopies have more changes over a shorter distance than the longer ones, indicating they are too short. This requires more work out of the air than it can give, resulting in the bigger region of low velocity behind the canopy in figures 2.6-2.8.

Referring to the 1400mm length canopy at 2900 and 3150 in figure 2.11 and 2.13, the 'bunching' of the lines seems similar, yet the peak negative C_p value is lower at the 3150mm canopy position. This reduction in $-C_p$ indicates less lift and in turn less drag as shown in the Force report in table 2.2 which is highlighted in red.

Turbulence

Without going into too much detail, investigating the turbulence on the surface will give as much additional information about how efficient the shape of the canopy is as the surface pressure plots do. Basically turbulence arises due to unsteadiness of the flow, it can be good; mixing the flow for heat exchange or mixing the boundary layer to delay flow separation and it can be bad; on a simple airfoil like the main wing. However for such a streamlined shape ideally an increased level of turbulence and a messy, large region of low turbulence towards the rear can be thought of as a loss particularly when there is a fast drop; a rapid loss of energy. There are a few key

points when looking at the turbulence plots in figures 2.9 to 2.13.

- 1) It is low where the stagnation point is at the front of the canopy, there is less unsteadiness as the fluid in this region is trapped and cant move
- 2) It is high between the thickest part of the canopy and the stagnation point. The region where the curvature is greatest causes the highest unsteadiness as the fluid pushes out and around the body and has to interact with the fluid adjacent to it and causes the adjacent fluid particle to also move. Thus it is clear the more blunt the front of the canopy is the more turbulence results as the curvature is higher.
- 3) The end of the canopy is messy with high and low regions of turbulence level. We are looking down on a 3D object, the sides of the canopy at the rearward tip are steep where as the top spine of it is not as severe. Ideally this low region would be smaller and more consistent, however it shows that there is a region of flow at the back of the canopy which is a little “over-worked” or stalled. It is not exactly separated and causing some drag, it could be refined a little more for a slight drag improvement.

Apart from the little stalled region towards the tip of the canopy the flow quality over it is reasonably good. There is no separation, which would be indicated by a large jump or some instability in the plot of pressure coefficient and turbulence. The final canopy length was based around the 1300mm long canopy shape, however the rear taper was extended marginally to assist in a smooth consistent pressure recovery. Obviously it was moved further back, however the individual force components for lift and drag of the final canopy alone are 0.1N and 4.7N respectively. Compared to the individual components listed in figures 2.9 - 2.13, the final lift and drag forces are a significant improvement.

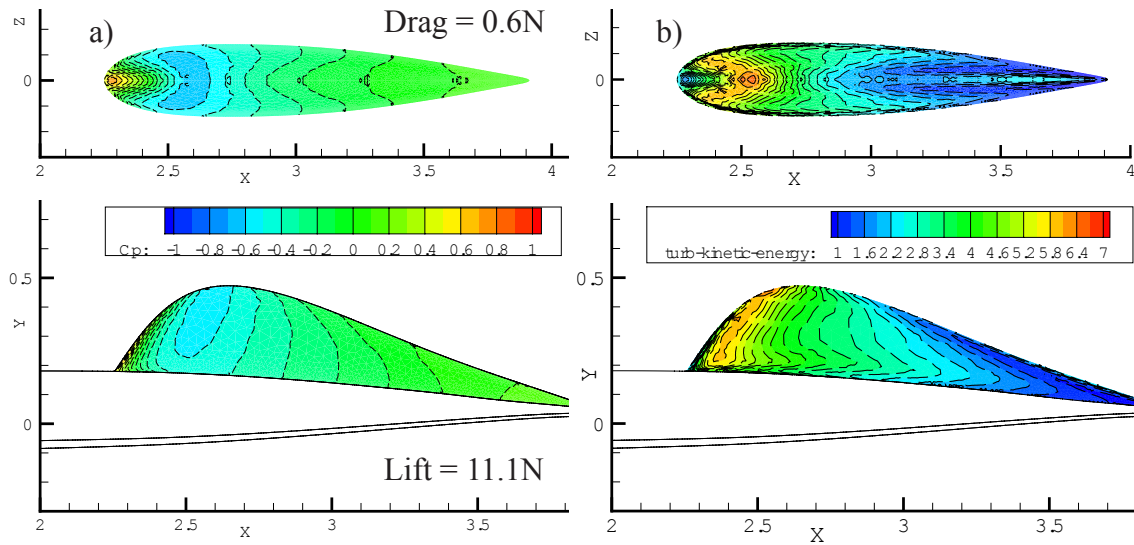


Figure 2.9 a) Pressure Coefficient and b) Turbulence for 2650-1800 Canopy with Forces

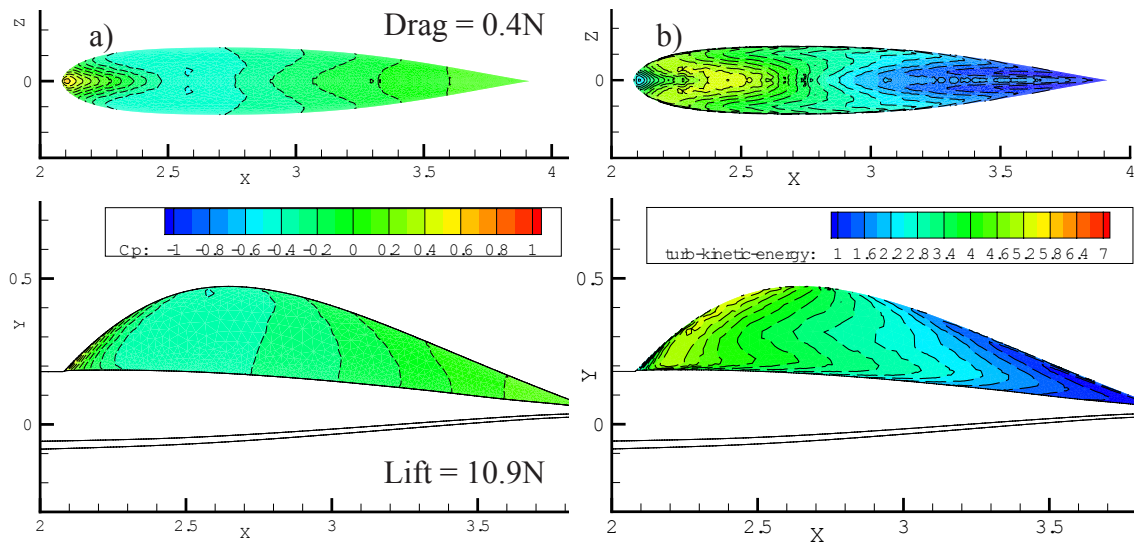


Figure 2.10 a) Pressure Coefficient and b) Turbulence for 2650-2000 Canopy with Forces

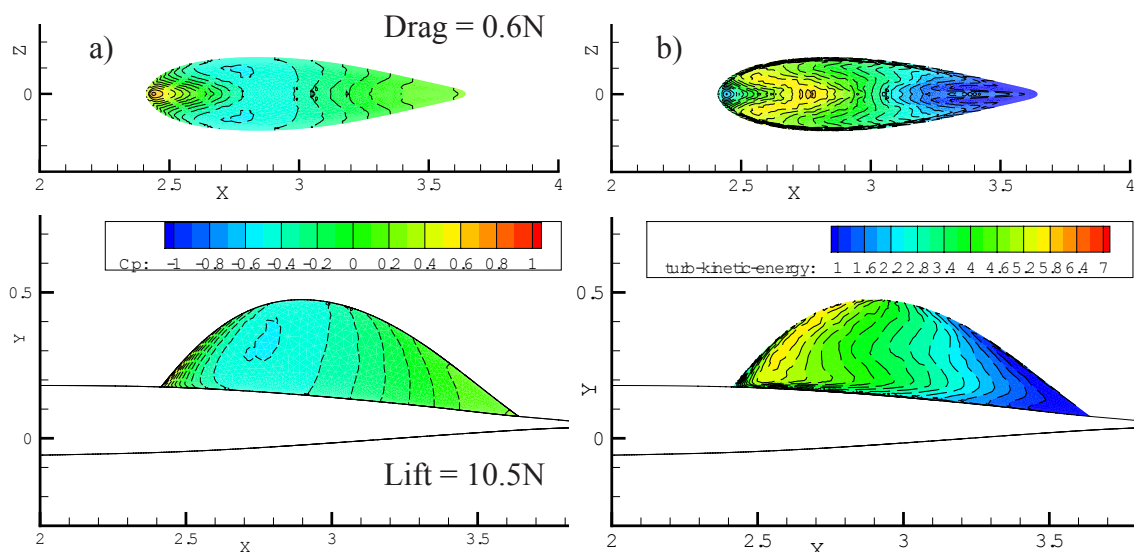


Figure 2.11 a) Pressure Coefficient and b) Turbulence for 2900-1400 Canopy with Forces

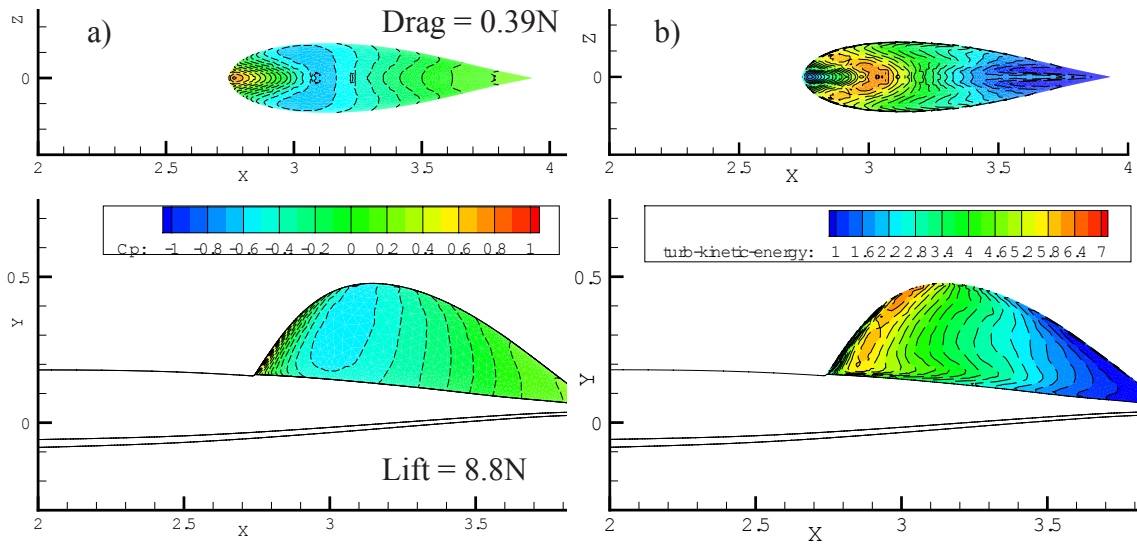


Figure 2.12 a) Pressure Coefficient and b) Turbulence for 3150-1300 Canopy with Forces

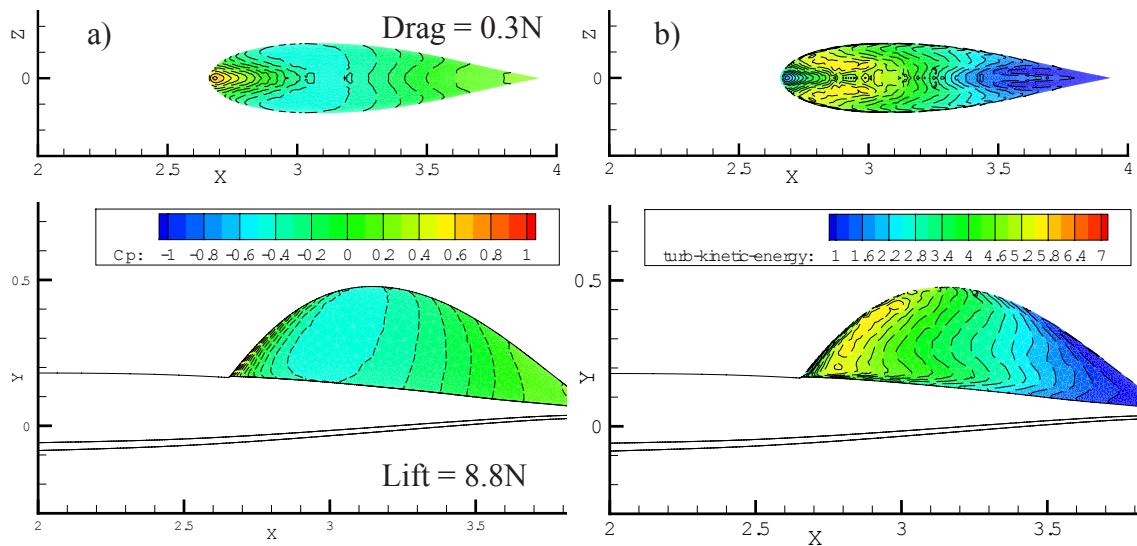


Figure 2.13 a) Pressure Coefficient and b) Turbulence for 3150-1400 Canopy with Forces

Bumpod Design

3

3.1 Introduction

The bumpod design had to capture all feasible positions that could locate the driver with respect to the canopy design locations previously studied. As this effectively locked in the location of the drivers hips (based off canopy position and 27° seating angle), the only parameters left to alter were the length of the bumpod and how much rear taper there should be. The front airfoil profile was based off a symmetric NACA 66 series airfoil, and scaled accordingly so that it was wide enough at the hip point. Due to this scaling the original aerodynamic data of the wing is invalid. However it is hoped that the leading edge shape of the bumpod is sufficient enough to promote attached flow to the majority of the bumpod, and not produce more turbulence or earlier transition than a more simplistic arc drawn by sight. It is expected that viscous forces would dominate the bumpod's drag, thus how short should it be such that there is no flow separation from the rear (governed primarily by the rear taper) and how far back it can be placed to accommodate the lower drag canopy towards the rear of the car as seen in the canopy design section.

3.2 Results

The three main canopy locations of 2650, 2900 and 3150 in chapter 2 were used to determine the longitudinal position of the bumpod. This was locked in by where the drivers hips would be located relative to the canopy and the 27° seating position. The bumpod length is referenced from the leading edge to the hip point (the widest point), additionally the distance to the trailing edge was varied from 100mm to 350mm to 600mm; effectively altering the rear taper ratio. The summarised drag history is plotted in figure 3.1, the raw data for all the configurations simulated can be found in figures 3.11, 3.12 and 3.13. Figure 3.1 however plots C_D against distance from the trailing edge of the car for a given bumpod length and canopy position. A lot of

configurations were tested (refer to figure 3.11 to 3.16 for full C_L and C_D), however the important ones are the 3150-1220 and the 2650-1220 bumpod geometries placed 100mm-350mm from the trailing edge. Both locations show that the drag curve is ‘flatter’ here, before increasing substantially to 0.127 for 3150-1220 at 600mm from the trailing edge; furthest towards the front of the car. Whilst the 2650-1220 results are marginally lower it is important to point out the composition of the drag forces here, see table 3.1.

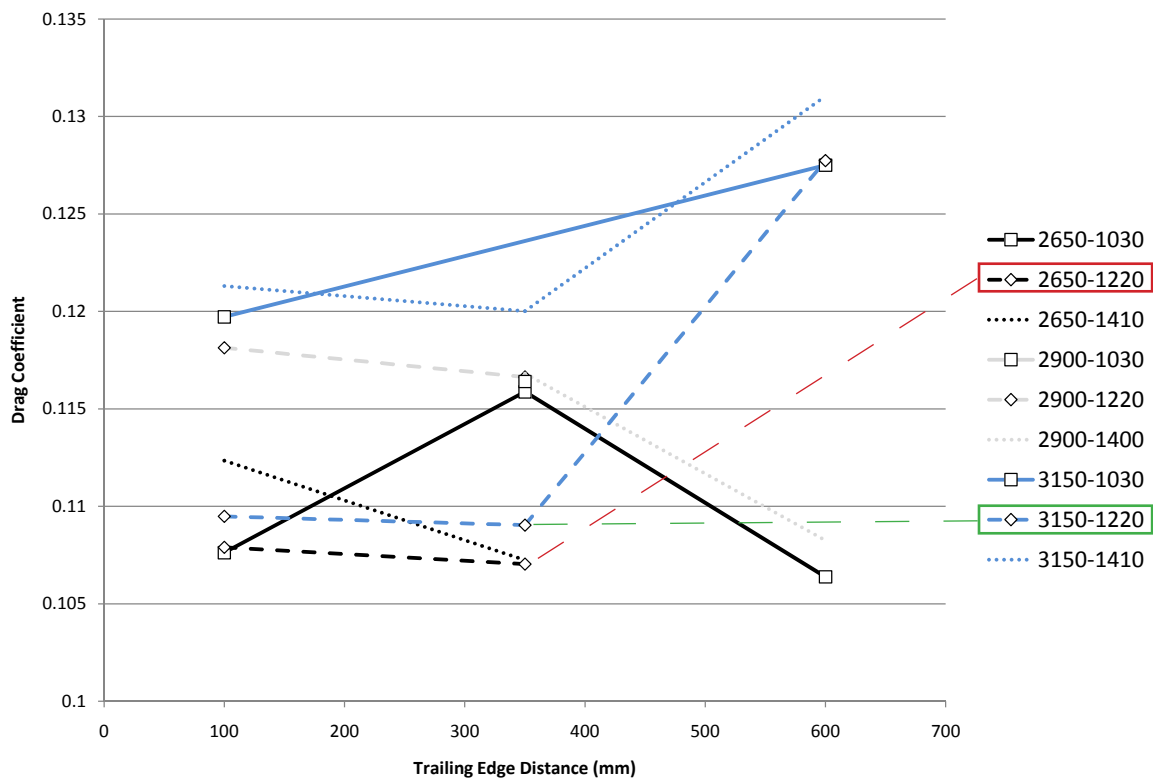


Figure 3.1 C_D versus Bumpod position from Trailing edge

There are two things of note, the first being that 3150-1220 case has lower viscous drag as its bumpod is significantly smaller, yet its canopy is ‘stumpier’ increasing it’s pressure drag component thus giving a marginally higher total drag. The second being that the further towards the rear the shorter bumpod is placed the lower and flatter the drag curve is. The 3150-1220 bumpod at 600mm has a higher drag than its 100mm and 350mm placement, so too in figure 3.1 does the 2900-1400-350 from 3150-1220 at 100mm (which is the nearly the exact same bumpod and canopy slid forward), see figure 3.5 and 3.8..

Table 3.1 Bumpod Design Total Car Viscous and Pressure Drag Composition

Component	Bumpod	100	350	600
Total	2650-1220	$C_D = 0.107$	$C_D = 0.106$	-
Viscous		76.9%	76.8%	-
Pressure		23.1%	23.2%	-
Total	3150-1220	$C_D = 0.108$	$C_D = 0.109$	$C_D = 0.127$
Viscous		74.6%	74.3%	68.4%
Pressure		25.4%	25.7%	31.6%

Figures 3.2 to 3.10 plot the pressure and turbulence over the surface of the bumpod. It is important to take note of the shape of the rear taper of the bumpod and how that effects the pressure and turbulence distribution towards the trailing edge. The bumpod geometries with more abrupt taper (see figure 3.7) ‘bunch’ up the bands of both turbulence and pressure contour, which means that the curvature is too sharp and the resulting adverse pressure gradient would tend towards flow separation (and increased pressure drag). Some may look extreme, however it is of concern to the overall packaging of the rear this was done until the final version of the bumpod was extended off the rear of the car to regain the lower taper ratio. The 2650-1030-350 bumpod in figure 3.3 has higher drag with canopy further forward even though C_p plot on bumpod seems reasonable. The increased length means the viscous drag dominates as in the drag component break down in table 3.1 for 2650-1220. Thus there is a balance to be struck between pressure drag and viscous drag. The figures relating to the side view of the bumpod show a skewed C_p distribution in the fillet radius from the bumpod to the main wing section, which is from the flow interference of the two surfaces at right angles. The fillet radius was not optimised and could potentially have been bigger to reduce this effect and likely drag increase; however it is probably minimal.

The 2650-1030-600 bumpod has the lowest C_D and C_L for the shapes tested. The rear taper is visually quite acceptable given the C_p plot in figure 3.2a and, it is reasonably short compared to the 2650-1220-100 bumpod in figure 3.4. Thus a trade off for less viscous drag (1N less than the average) whilst ensuring pressure drag does not rise has been found, thus the 2650-1030-600 bumpod is the baseline for the final bumpod geometry.

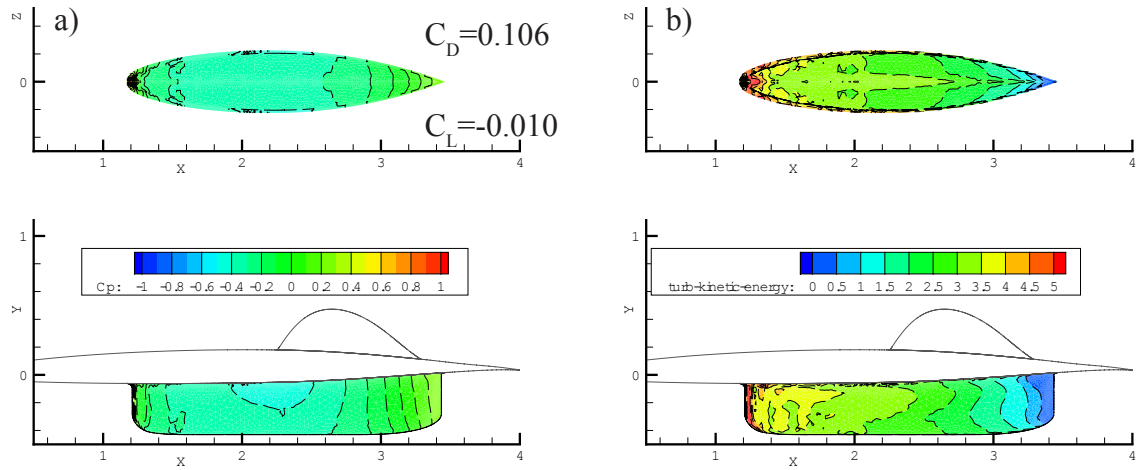


Figure 3.2 2650_1030_600 Bumpod Pressure and Turbulence Plot

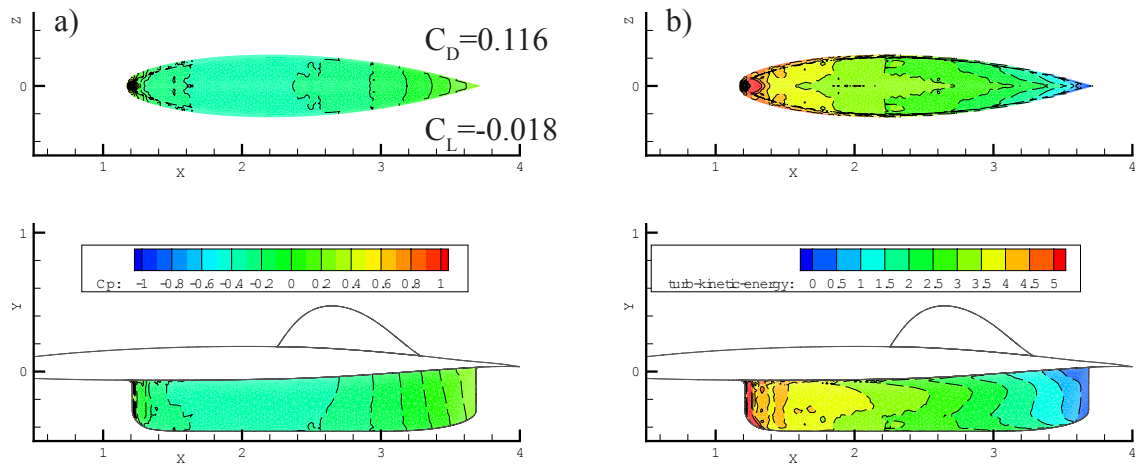


Figure 3.3 2650_1030_350 Bumpod Pressure and Turbulence Plot

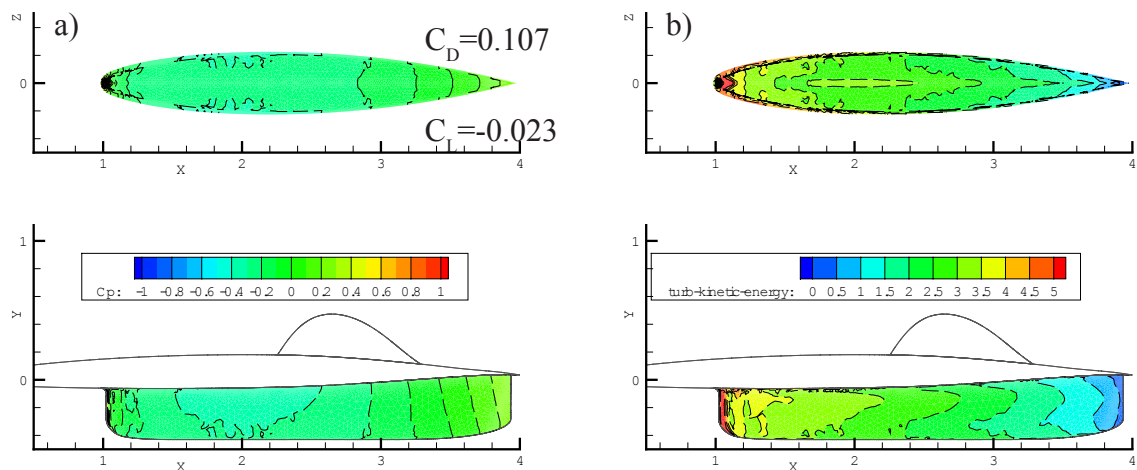


Figure 3.4 2650_1220_100 Bumpod Pressure and Turbulence Plot

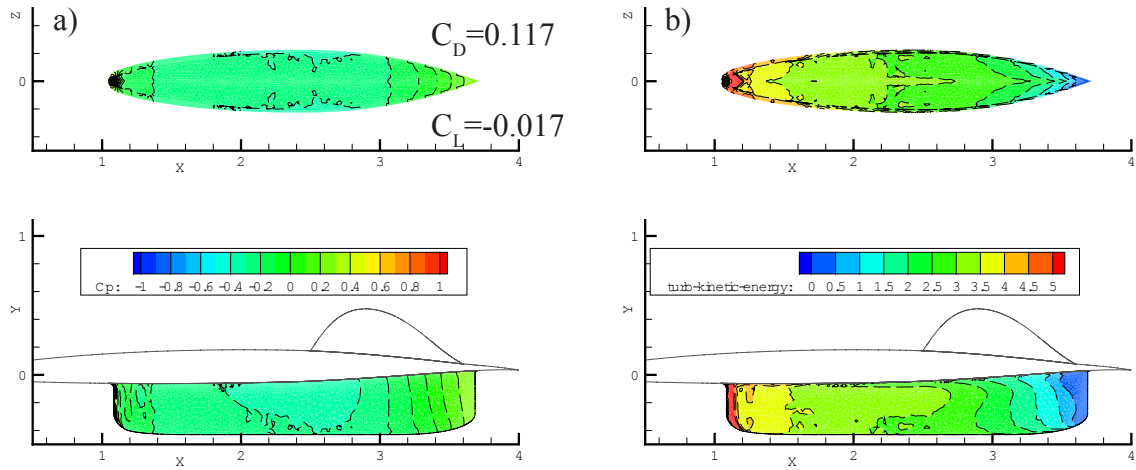


Figure 3.5 2900_1410_350 Bumpod Pressure and Turbulence Plot

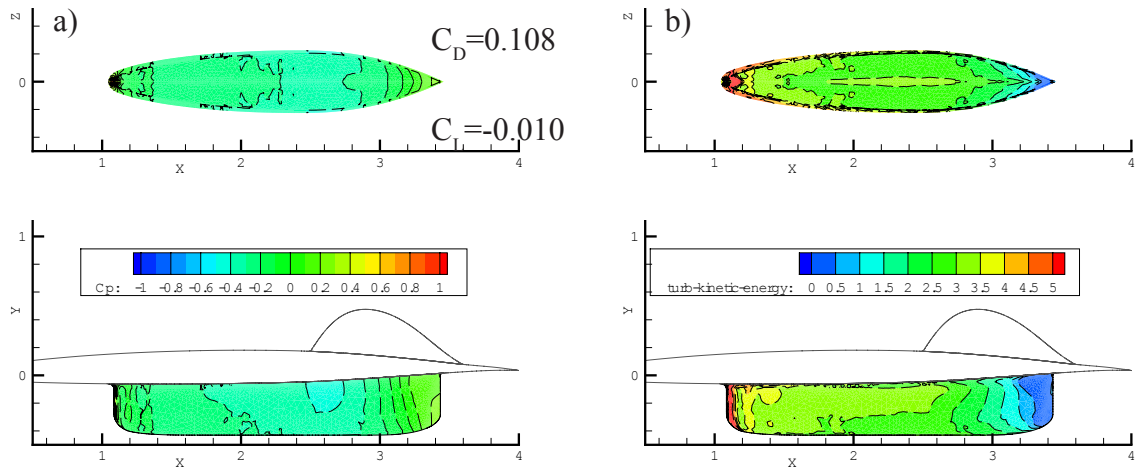


Figure 3.6 2900_1410_600 Bumpod Pressure and Turbulence Plot

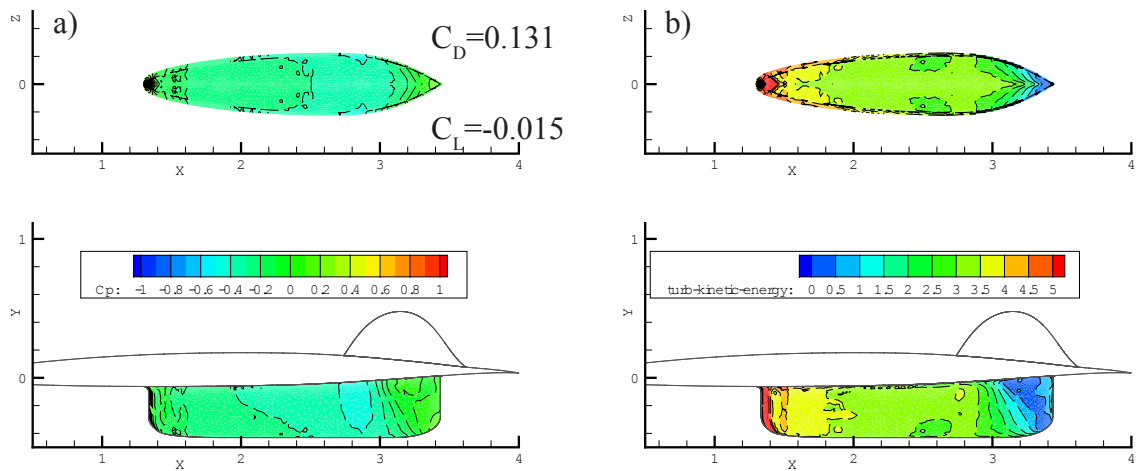


Figure 3.7 3150_1410_600 Bumpod Pressure and Turbulence Plot

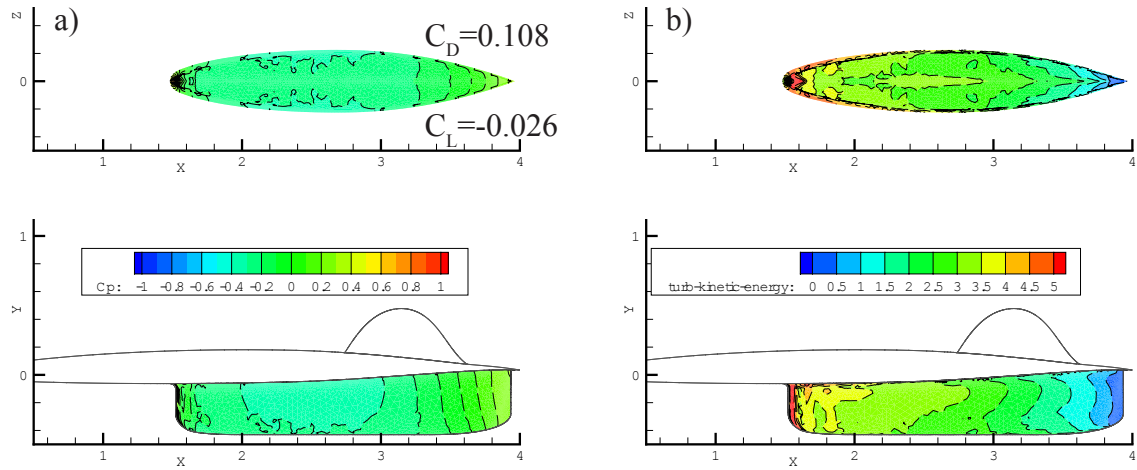


Figure 3.8 3150_1220_100 Bumpod Pressure and Turbulence Plot

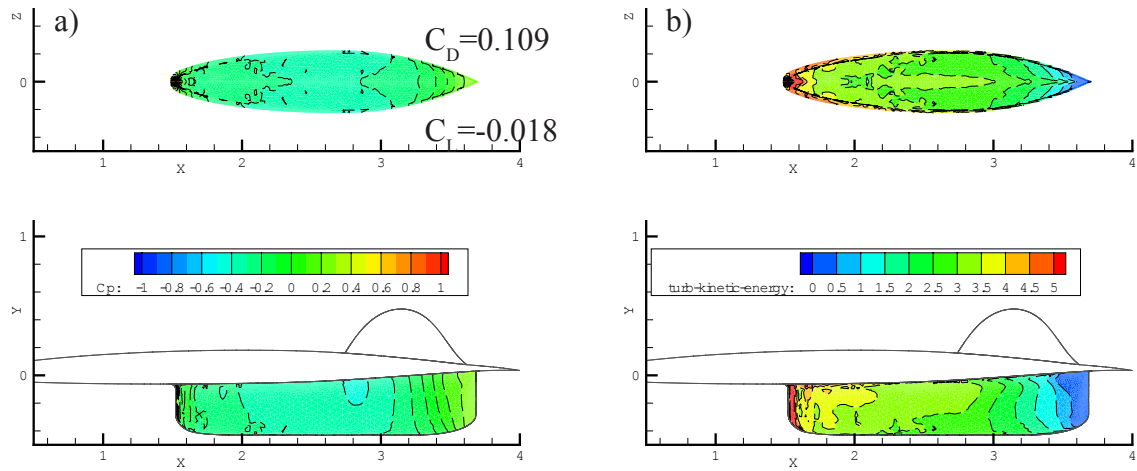


Figure 3.9 3150_1220_350 Bumpod Pressure and Turbulence Plot

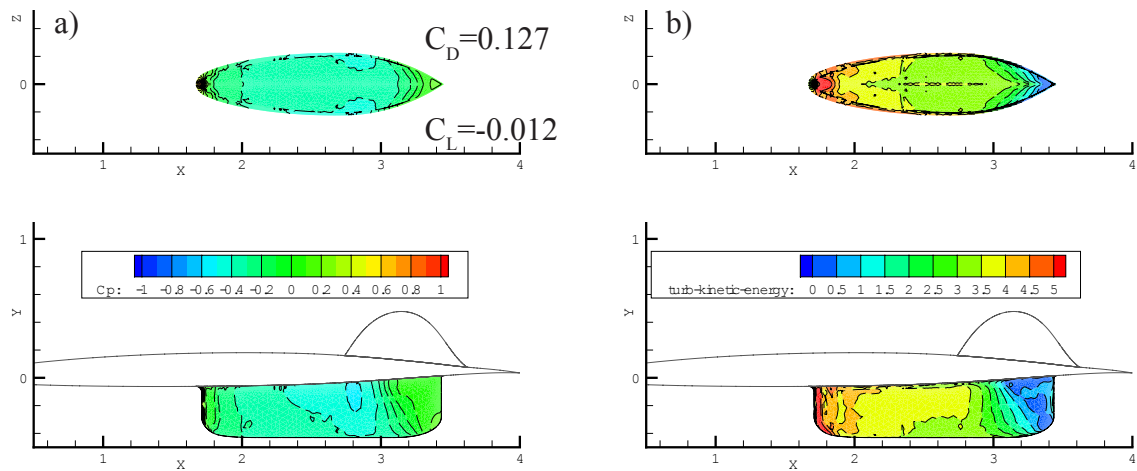


Figure 3.10 3150_1220_600 Bumpod Pressure and Turbulence Plot

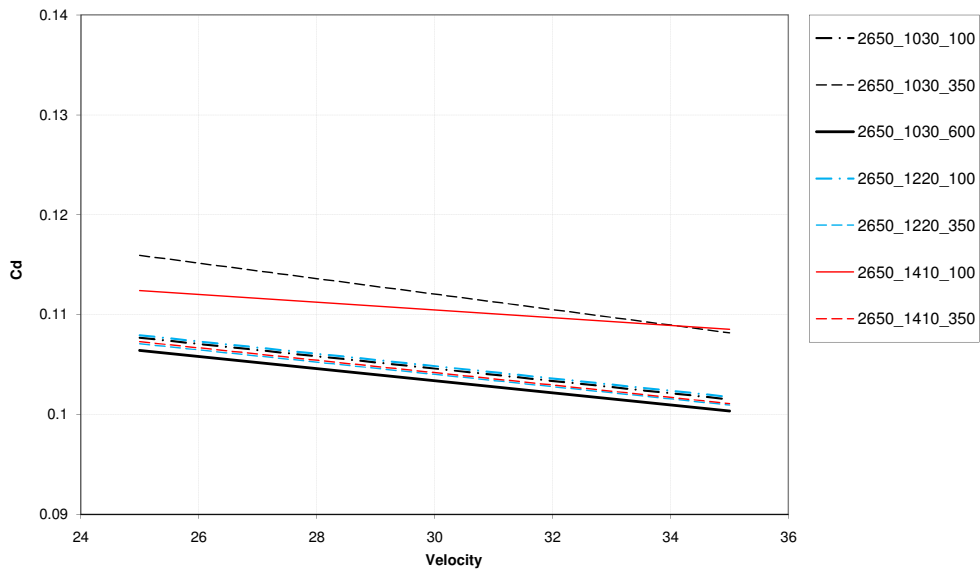


Figure 3.11 2650 Bumpod Configuration Drag Coefficient vs Speed

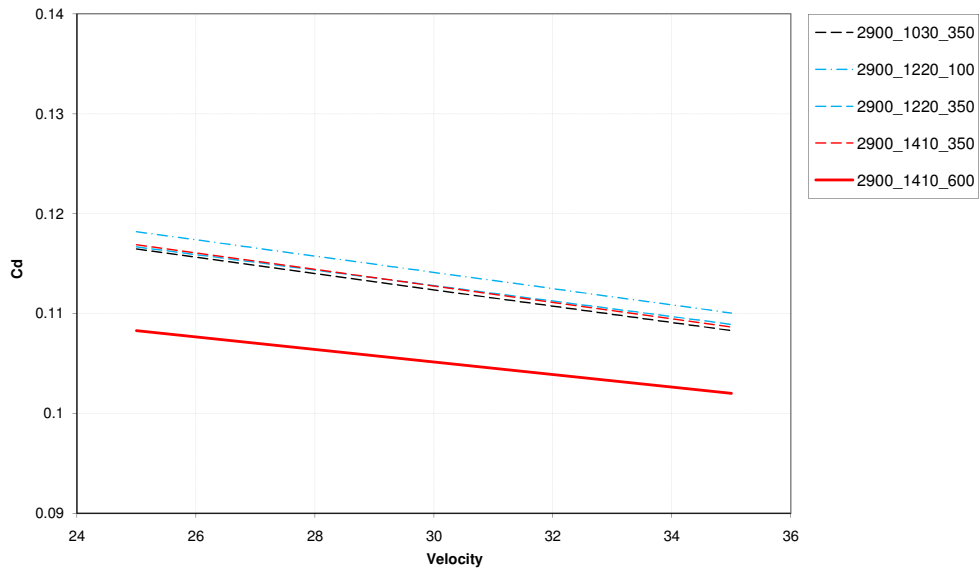


Figure 3.12 2900 Bumpod Configuration Drag Coefficient vs Speed

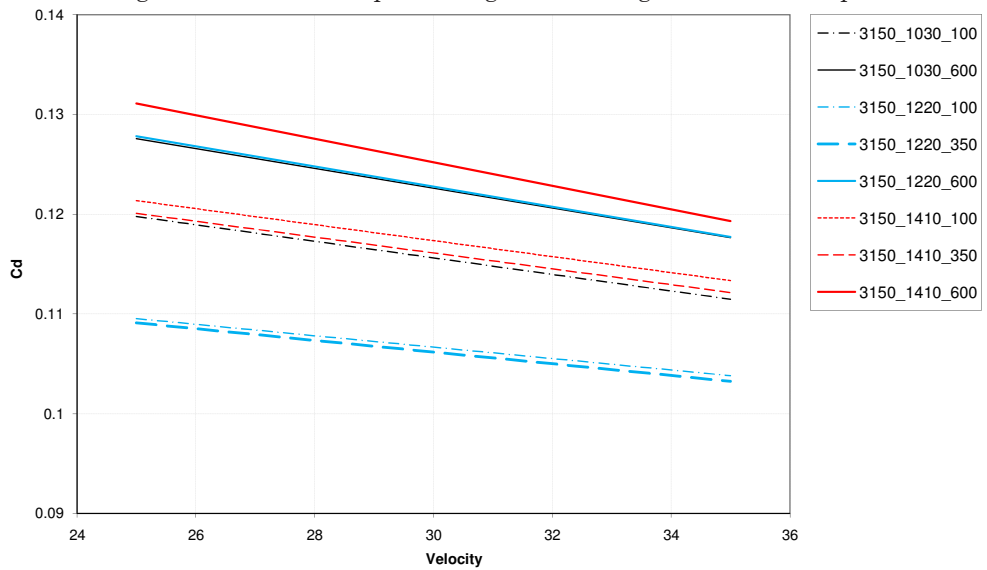


Figure 3.13 3150 Bumpod Configuration Drag Coefficient vs Speed

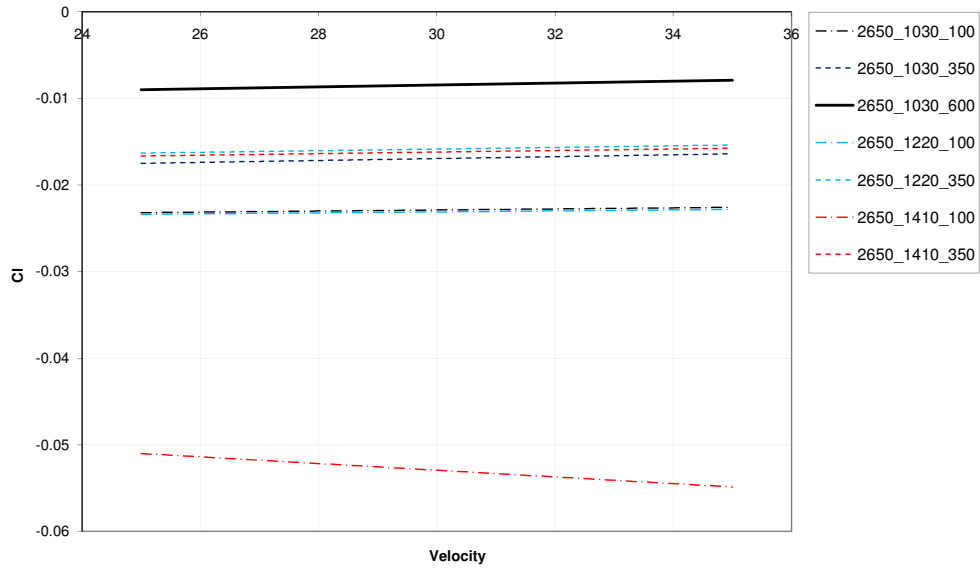


Figure 3.11 2650 Bumpod Configuration Lift Coefficient vs Speed

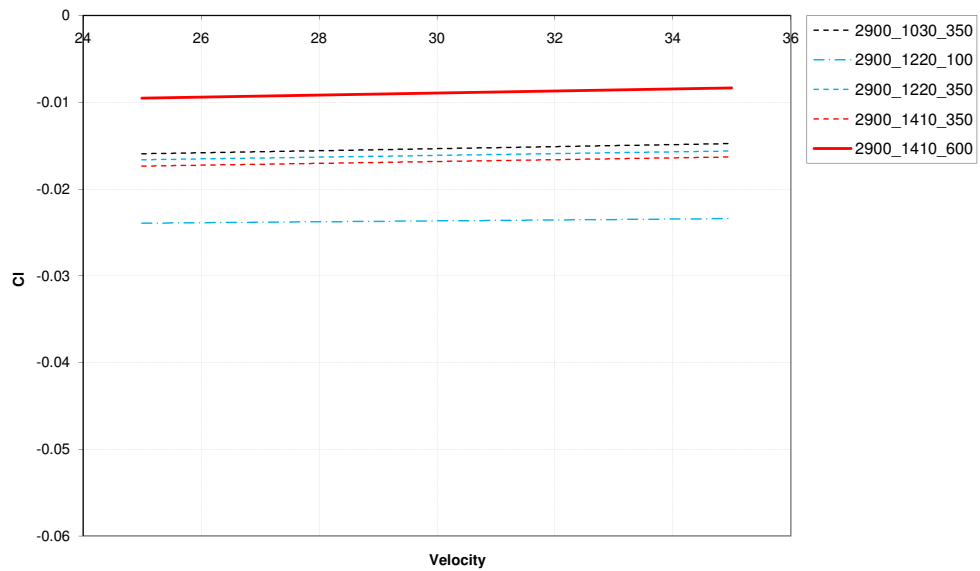


Figure 3.12 2900 Bumpod Configuration Lift Coefficient vs Speed

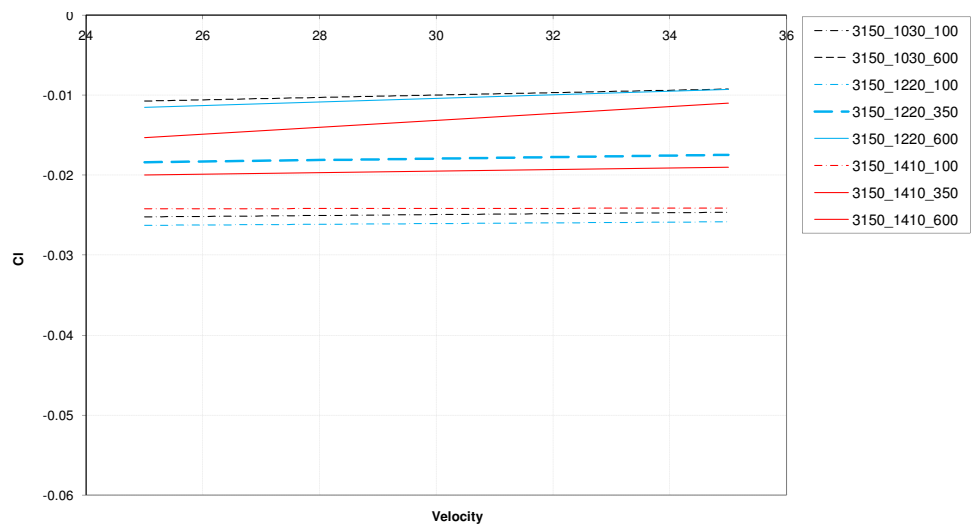


Figure 3.13 3150 Bumpod Configuration Lift Coefficient vs Speed

Wheel Fairings

4

4.1 Introduction

The actual fairings themselves were not aerodynamically optimised in this design study, as they were already designed for Sunswift 3. Thus the focus of the wheel fairing design centred on the location of the fairings with respect to the bumpod. Three longitudinal placements and three lateral placements were selected to determine the relationship of lift and drag with how far forward and how far outward from the bumpod they should be placed. The larger bumpod from the canopy study was used as the wheel fairing's placement would affect lift and drag more in this case. As the final bumpod will most likely be smaller and further rearward, it is reasonable to assume the net drag will reduce further. So in pure terms of establishing a relationship of the aerodynamic forces between the fairings and the bumpod, the assumption of studying the placement of the fairings with respect to the larger bumpod is satisfactory.

Table 4.1 Wheel Fairing Location

Configuration	Longitudinal position (X) mm	Outboard Position (Y) mm
1, 2, 3	150	550, 650, 750
4, 5, 6	650	550, 650, 750
7, 8, 9	1150	550, 650, 750

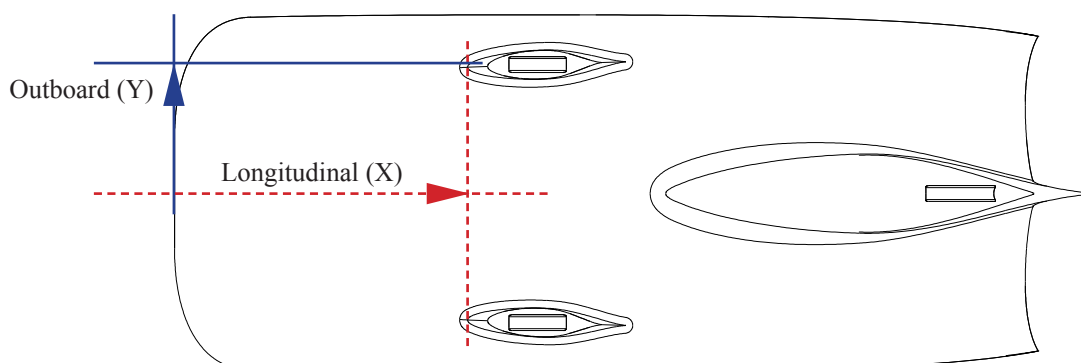
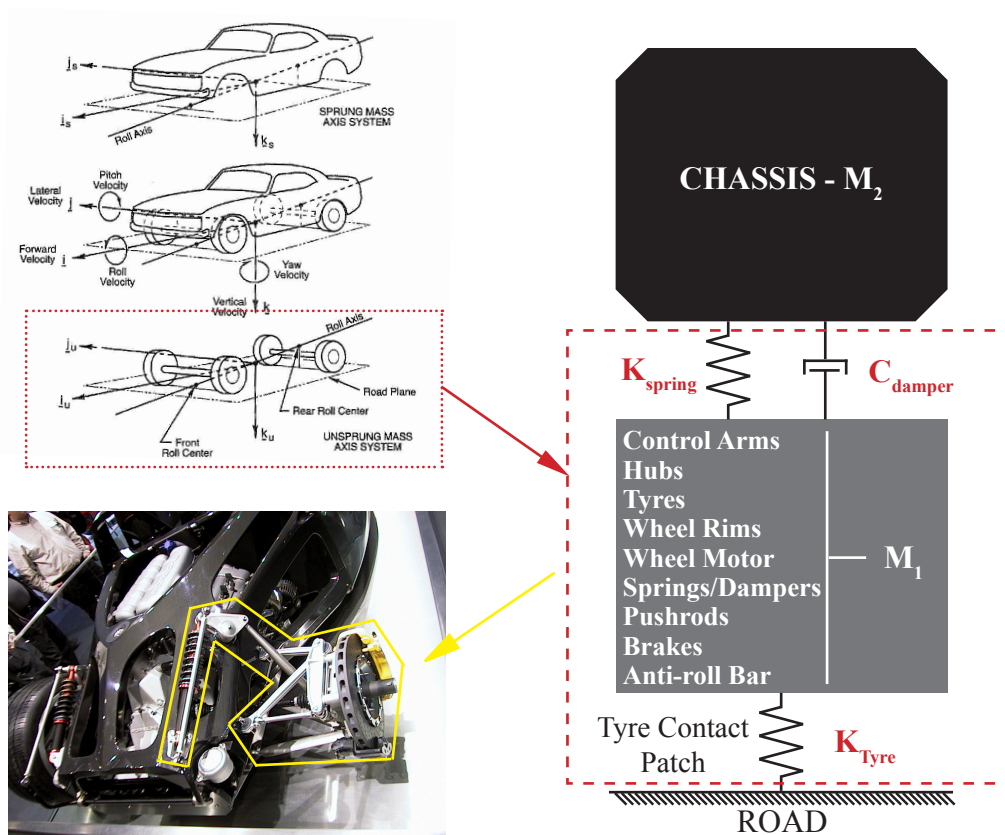


Figure 4.1 Wheel Fairing Location

The placements are listed in table 4.1, and figure 4.1 indicates the main parameters. Whilst the wheel placement based solely on aerodynamics may not be the best solution given suspension movement and travel, the resulting aerodynamic ‘map’ of lift and drag with these placements will allow a good compromise between aerodynamic concerns and mechanical grip (road holding). Structurally speaking, a shorter distance between the suspension pick up points on the chassis and the wheel itself will make for a lighter more robust suspension. The further out the wheel is the longer it will have to be and most likely heavier in order to take the stresses of a larger bending moment. Therefore weight saving is a third consideration, and considering it is ‘unsprung mass’ it is crucial that it’s kept light as possible. More detail can be found of its importance in vehicle dynamics text books such as Milliken and Milliken, however the lighter the unsprung mass is the more dynamically responsive a car will be. 3rd year vibrations in Mech Eng will start involving masses and springs in series which may make more sense of figure 2.



Unsprung mass without tyre highlighted in yellow
(Porsche Carrera GT Rear Suspension)

Figure 4.2 Simplified Mathematical Suspension Model

4.2 Results

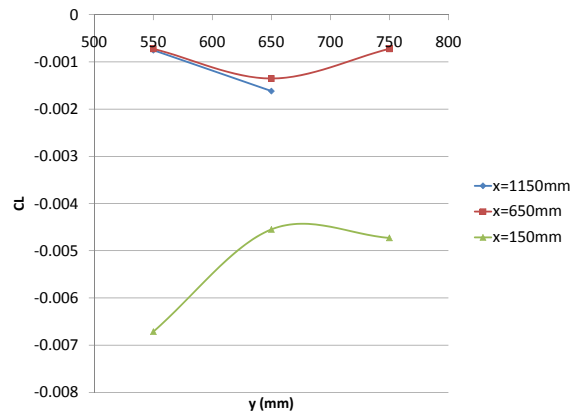


Figure 4.3 Wheel Fairing Placement Effect on Lift Coefficient

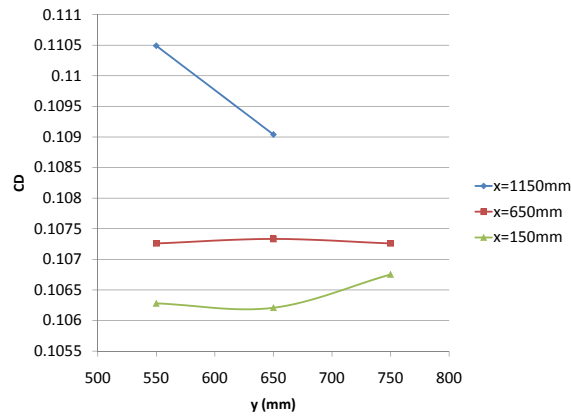


Figure 4.4 Wheel Fairing Placement Effect on Drag Coefficient

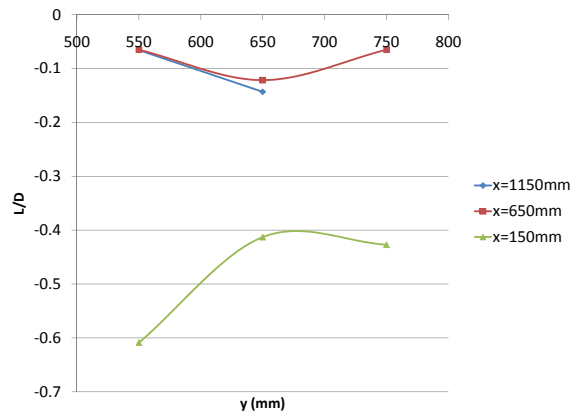


Figure 4.5 Wheel Fairing Placement Effect on Aerodynamic Efficiency

The lift, drag and aerodynamic efficiency are shown in figures 4.3, 4.4 and 4.5 respectively. Some configurations did not yield results due to file corruption etc., but the main trends and conclusions that are of importance can be determined. Namely that the further away from the bumpod the fairing is placed, the lower the overall drag of the car is. There is slight increase for $y=750\text{mm}$ at $x=150\text{mm}$ (as there would be an interaction with the flow around the front corner of the car and then straight onto the spat). There is little variation in drag for the lateral placement at $x=650\text{mm}$,

however the closest the fairing is placed to the bumpod at $x=1150\text{mm}$, $y=550\text{mm}$ results in the highest drag. However drag is not the only concern, lift is also as important and we can see that at $x=650\text{mm}$ the fairing placement is quite neutral (i.e. $C_L \approx 0$), whereas the car has more downforce at $x=150\text{mm}$. This is due to the fairings acting as endplates, speeding up the air flow even more at the part of the car closest to the ground; $-C_p$ to act over a greater area under the car (see the linked C_p bands in figure 4.6). Thus for the least impact on the aerodynamic balance the positioning around $x=650\text{mm}$ will be the most suitable.

Pressure Coefficient

As the fairings move outward, it is noticeable that the pressure distribution around the side of the fairing acting on the underbody is contained at 550 and 650, whereas at 750 the lower pressure coefficient 'spills' up and around the side rails of the car. When the fairings are placed at 650mm along the car in figure 4.7, the high pressure areas around the front of the bumpod and fairings and low pressure areas at the side of the bumpod and fairings seem balanced, which contribute to the neutral lift of the car. At $x=1150\text{mm}$ fairing placement the low pressure areas at the side of the fairings and the bumpod is now 'joined' due to the narrower gap between them which inturn increases their affect on each other, the same can be said for the now larger region of higher pressure that link all three stagnation points of the two fairings and the bumpod.

Turbulence

The Turbulence shows that the further forward the fairings are placed, the higher the turbulence distribution in the immediate vicinity under the leading edge of the car is, and the further out the fairing is placed at $x=150\text{mm}$, the greater the downstream 'trail' of turbulent flow acts on the side rail of the car. This is due to the positioning of the fairings accelerating the flow under the car and inturn increasing the downforce, so right at the front may not be best. At $x=650\text{mm}$ the turbulence distribution seems a little lower around the sides of the fairing and in the gap between each fairing, this would be expected as there is less lift in this case, there is less energy being taken out of the flow in order to produce a force. However when the fairing is placed at $x=1150\text{mm}$, the changes and the distribution of the turbulence on the underbody seem more severe, as is the increased turbulence behind the wheel fairings and on the front part of the bumpod, clearly this is due to the increased interaction between the three protrusions and highlights the concept of interference drag both in the

surface plot of turbulence and the force report in figure 4.4. The rear turbulence also changes when the fairings are in the most rearward position as the accelerated flow between the fairings and the bumpod place a different ‘pressure recovery’ demand on the shape of the rear of the whole car.

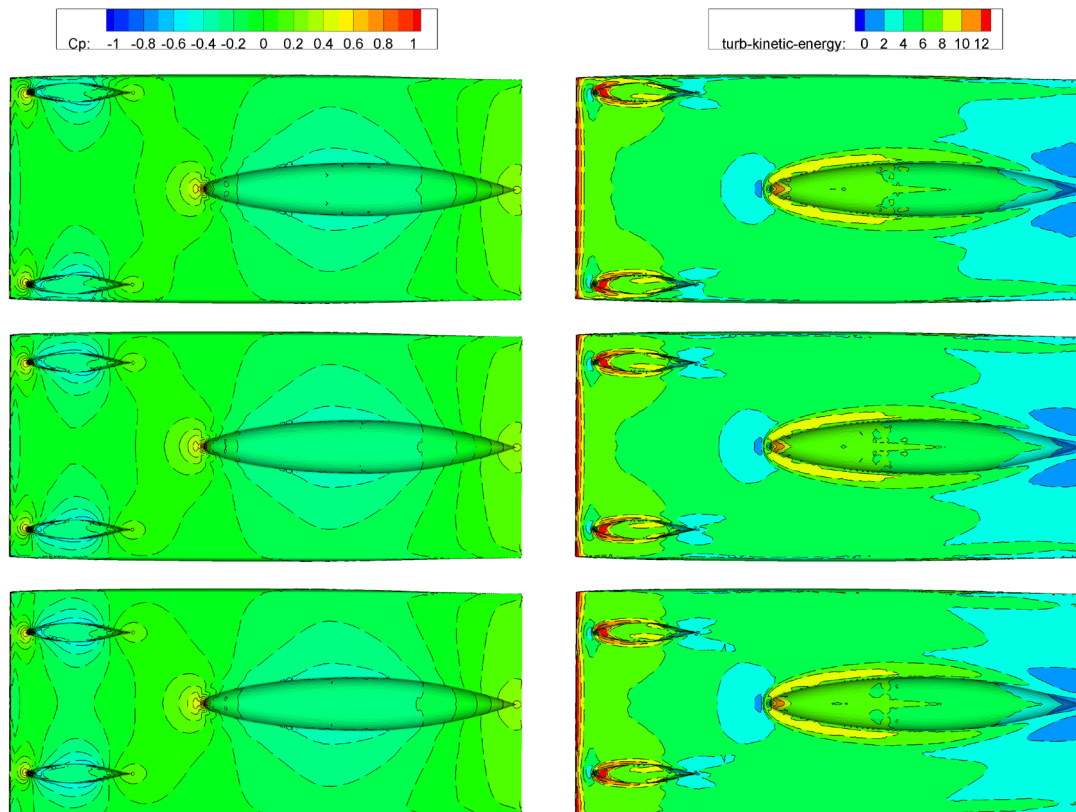


Figure 4.6 Wheel Fairing Placement Pressure and Turbulence Plots at $x=150\text{mm}$

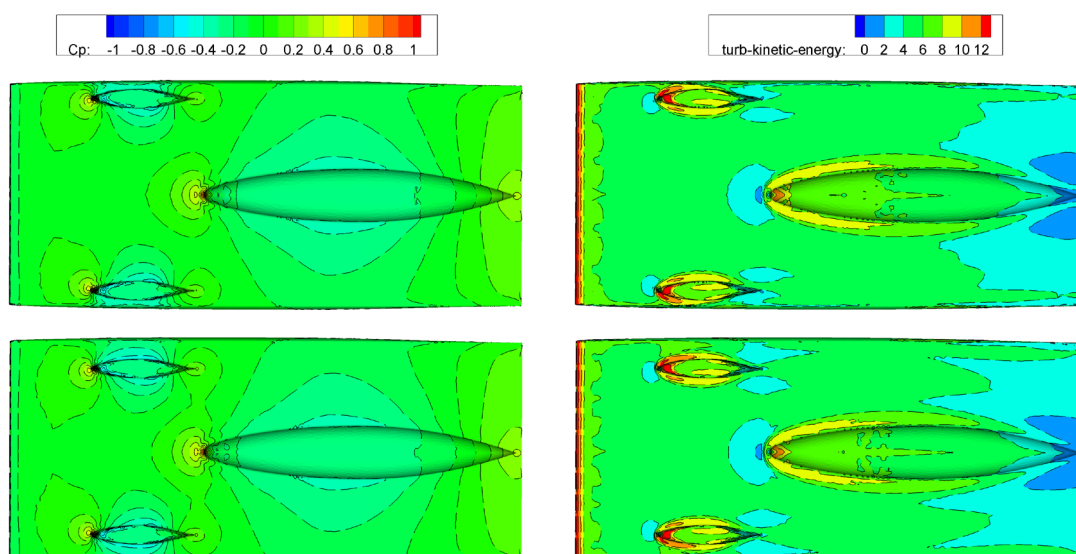


Figure 4.7 Wheel Fairing Placement Pressure and Turbulence Plots at $x=650\text{mm}$

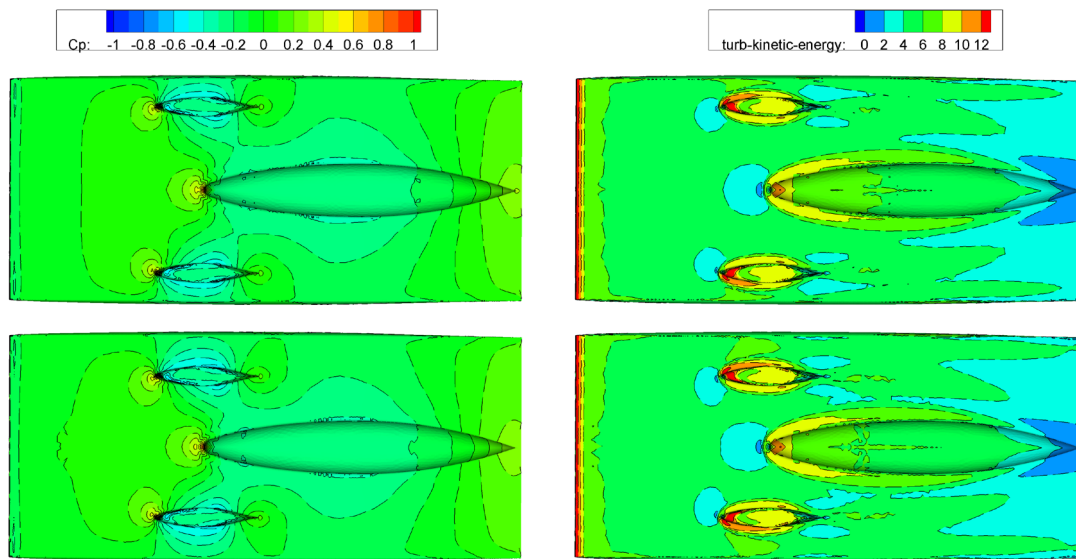


Figure 4.8 Wheel Fairing Placement Pressure and Turbulence Plots at $x=1150\text{mm}$

Undercar Flow Plane

The flow visualisation plane located half between the ground and the underbody in figures 4.9 to 4.11 shows the wake behind the fairings gets shorter the closer towards the bumpod they are placed, whilst at the same time the high speed flow around the side of the bumpod reduces. While it is not as obvious, the wake behind the bumpod grows as the fairings are placed at $x=1150\text{mm}$. The turbulence behind the fairing also increases in thickness and intensity (marginally) and the 'trail' behind it is shorter as its is influenced by the bumpod, it is also sucked in around the back of the bumpod more noticeably than the 'straight' trail the wake leaves behind the fairing at $x=150\text{mm}$.

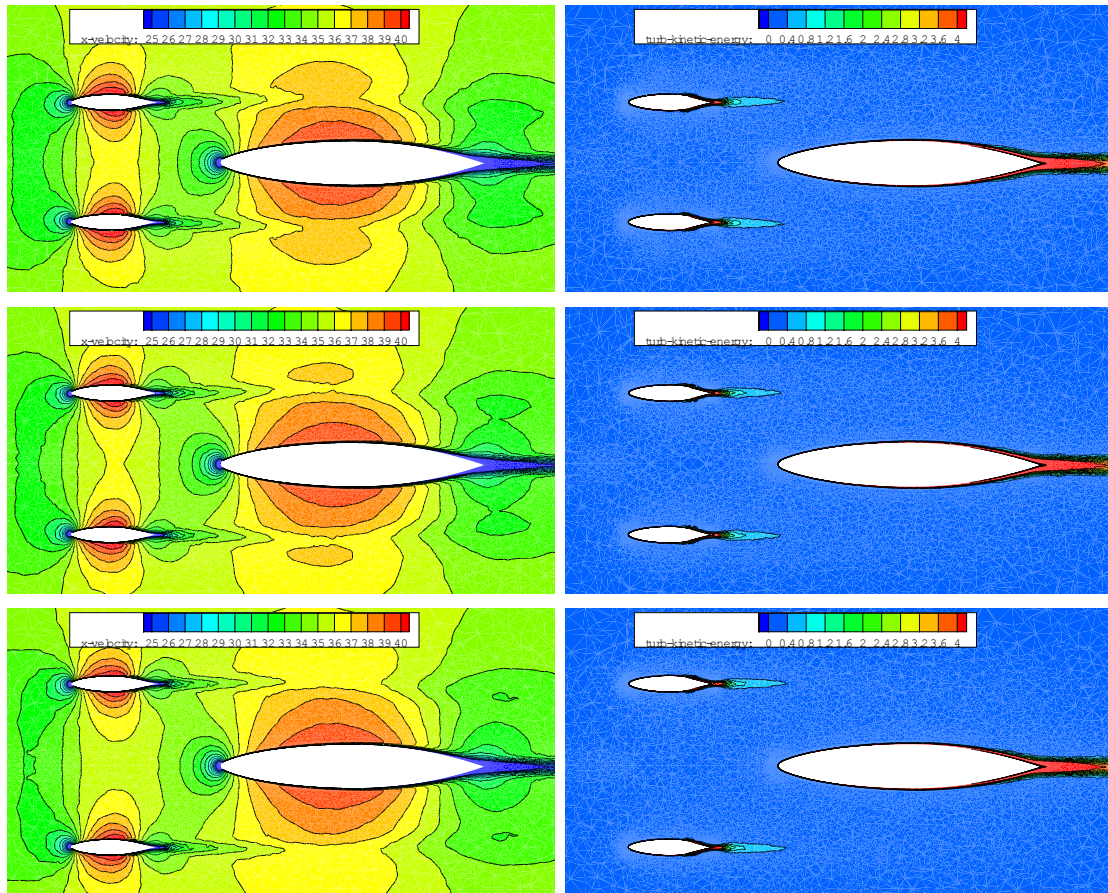


Figure 4.9 Wheel Fairing Placement Pressure and Turbulence Plots at $x=150\text{mm}$ undercar flow plane

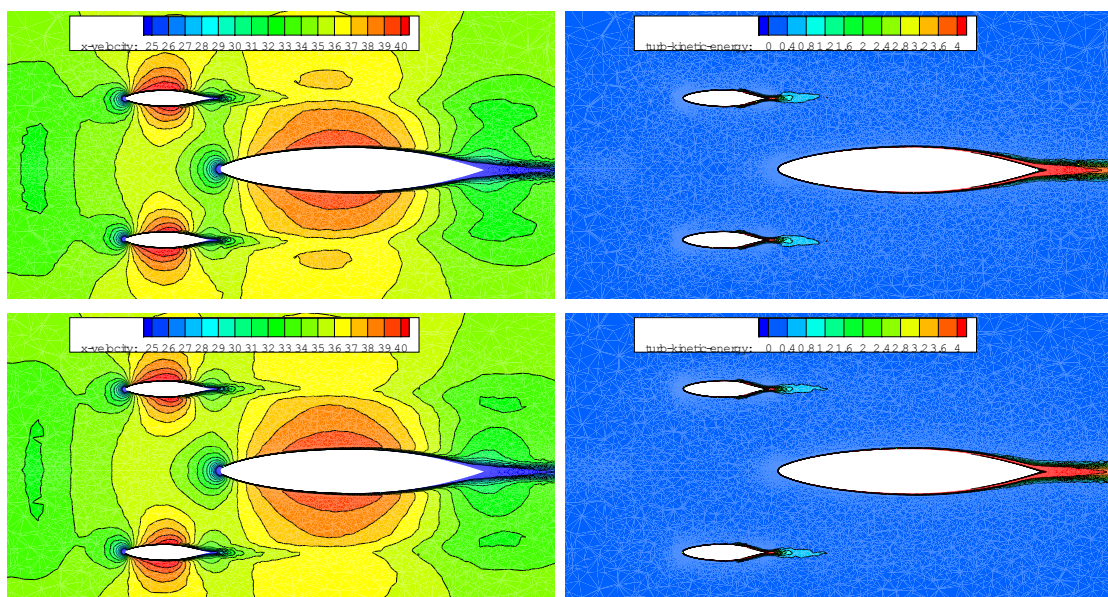


Figure 4.10 Wheel Fairing Placement Pressure and Turbulence Plots at $x=650\text{mm}$ undercar flow plane

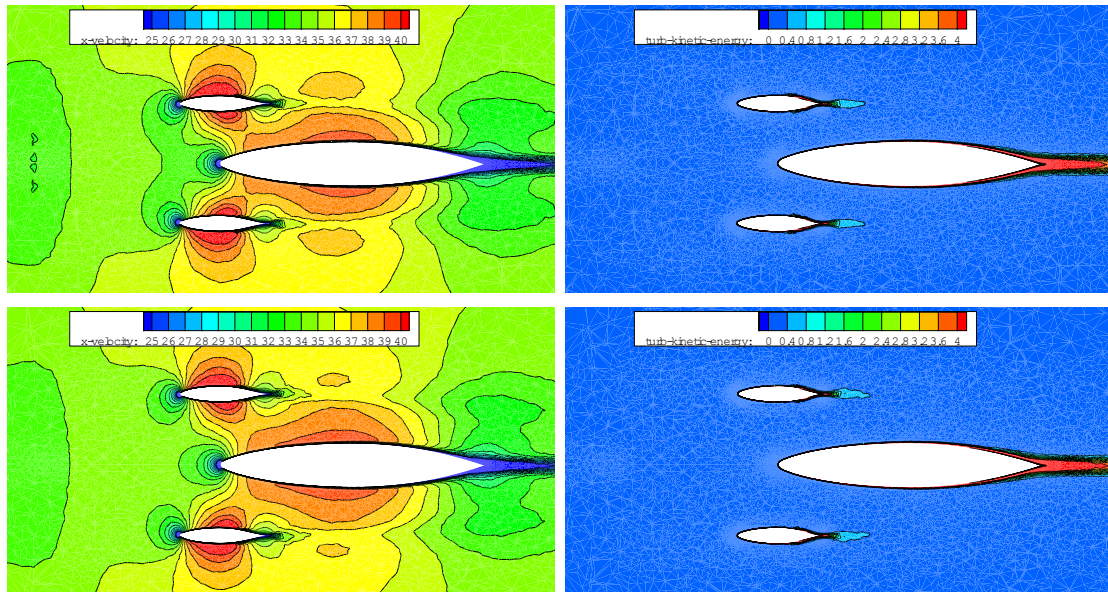


Figure 4.11 Wheel Fairing Placement Pressure and Turbulence Plots at $x=1150\text{mm}$ undercar flow plane

Summary

Thus knowing the placement of the spats is most aerodynamically 'neutral' at around $x=650$, this region will be the target of the fairing location, indeed the final fairing location will coincide with the maximum thickness of the main body airfoil section so that the maximum 'mechanical envelope' of the suspension travel can be utilized. There appears to be no straight line benefit of the placement at the most outboard location of the fairings (like Nuna5), and indeed may have additional adverse affects when the car is in a cross wind, as there is a vortex produced by the fairing and the underbody (as most 90° 'bluff' protrusions from a surface do). In a cross wind this could potentially migrate up and around to the top surface of the car, causing additional interference drag. Thus the slightly inboard location may assist with keeping this vortex under the car. Also as the wheels/fairing are integrated and 'steer', keeping the fairing flush with the underside at all times is important. Leaving the fairing just short of the side rail of the car will make it possible to have $\approx \pm 10^\circ$ of steering lock without the fairing and the integrated fairing fillet coming away from the underbody too much.

Aerodynamic Analysis of IVy

5

5.1 Introduction

The step forward from the previous work relating to the canopy, bumpod and wheel fairing placement required a few additional refinement steps be carried out at once. With no time to conduct a full parametric analysis in CFD of these details, instinct and experience was relied upon to jump forward on the ever tightening time frame. The following steps were taken:

- Lower airfoil surface (NACA 66-209) was re-profiled thinner and flatter
- Static -1.5 degree dive on wing for slight downforce
- 2 degrees ‘toe-in’ on wheel fairings to get some ‘sail’ out of them
- Front corner rounding to minimise sharp corner producing vortices in yaw
- Side rails rounded and array surface angled to limit adverse effects in yaw
- Canopy refinement
- Bat-Wing trailing edge
- Slight bumpod narrowing and draft angle given for mould release
- Bumpod leading edge angled to reduce turbulence in forward radius.

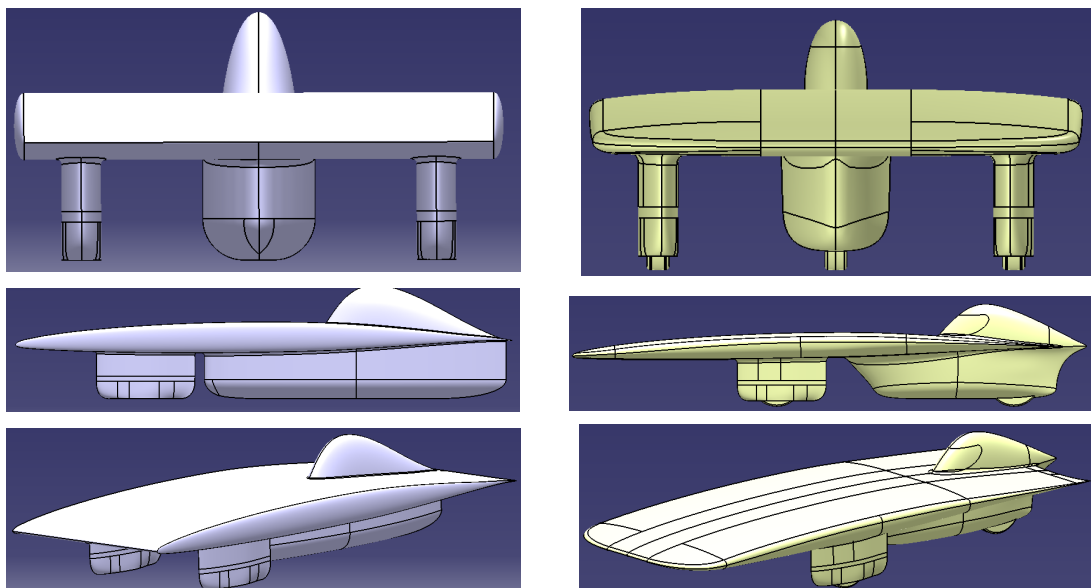


Figure 5.1 Comparison of “Lunchbox” preliminary version and final IVy

Importance was placed on making sure the car was stable at speed, thus the decision to run a 1.5 degree angle to induce some downforce as a margin of safety was considered wise, however the drag penalty is not too severe. As the old saying goes in order to finish first, first you must finish. Considering it can be quite gusty in the desert it is quite possible with the wrong gust of wind the car would become light on steering at the wrong time. Given the earlier discussion on CFD mesh uncertainty in Chapter 1, the meshes for all the cases here are identical as the same file was used but different velocity inputs were given. So even if the outright values may have some error in them, as the mesh is consistent the trends of the results should hold up against other form of measurement. For the CFD analysis a k-epsilon Realizable turbulence model was used, and 0, 10, 20 and 30 degrees of yaw was investigated at 70 km/h 90 km/h, 110 km/h ,130 km/h and 200 km/h. These speeds are not unreasonable given some gusts can get up that high instantaneously and in excess of the top speed of the car.

5.2 Results

5.2.1 Aerodynamic Force Map

The data in figure 5.2 shows the drag coefficient for the car from 0 degrees yaw to 30 degrees yaw for the given velocity range. The drag force result might seem confusing at first as C_D tends to reduce with increasing velocity for all angles of attack. This is not saying the drag force is reducing, but is merely for most subsonic shapes as the velocity is increased the drag coefficient will reduce then plateau (as for 0 yaw 30=60m/sec), as drag forces in the laminar range are always quite high. From 0 degrees yaw to 10 degrees yaw there is a small increase in C_D , which can be explained as the slight angle 'sees' more of the car than the other two yawed configurations. It effectively hits the two wheel fairings and the bumpod underneath the car equally. However at higher angles the windward wheel fairing starts to deflect the flow onto the bumpod, so there is less drag being generated by the bumpod. Additionally the drag reduction with increased yaw is being traded off against a sharp rise in the side force, not that the car suddenly is working better.

Table 5.1 Aerodynamic Properties of IVy at 0 yaw

Speed	C_D	C_L
70 km/h	0.131	-0.039
110 km/h	0.109	-0.098
Area Component	0.63 m ²	6.92 m ²

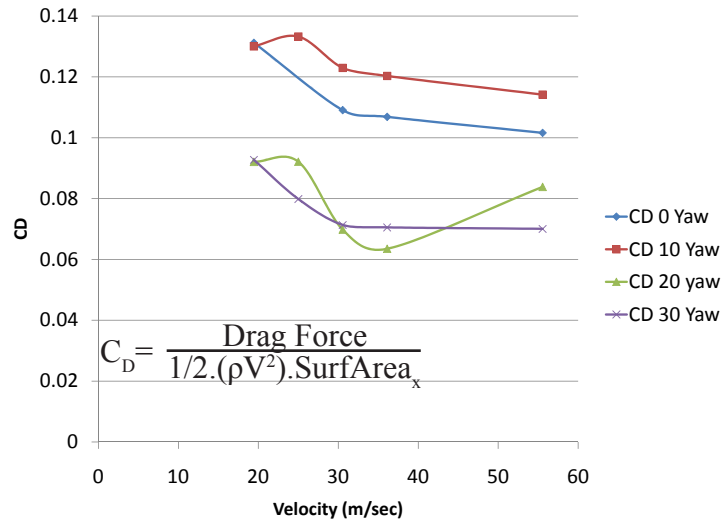


Figure 5.2 C_D Aero Map for IVy (DRAG)

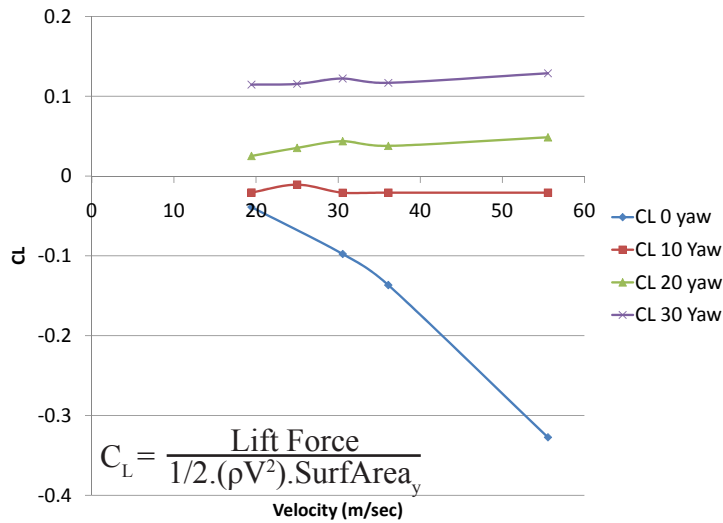


Figure 5.3 C_L Aero Map for IVy (LIFT)

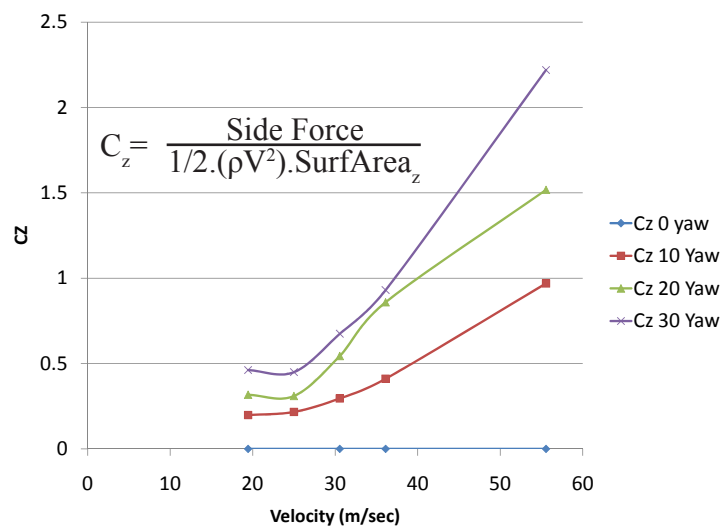


Figure 5.4 C_z Aero Map for IVy (SIDE FORCE)

The lift coefficient in figure 5.3 shows the downforce generating ability of the car at its designed -1.5 dive angle. It indicates how efficient the shape is that C_L rapidly decreases for not much increase in drag. The only increase in C_L occurs when the car is in yaw. This happens due to the once low pressure under the car as the air is accelerated underneath easily flows around the streamlined bumpod and wheel fairings is now substantially more blocked by them. This generates higher pressure acting over a bigger area, effectively eating into where the low pressure was and increasing the lift. Starting out at “neutral lift” from a 0 dive angle would have made this worse, at least that for a few angles outside of 0 degrees the car will be stable, perhaps indicating the Bat-Wing at work.

The side force coefficient in figure 5.4 is a little more self explanatory. Obviously as the cross flow velocity component increases on the side area (of 1.95m^2) this increases quickly. *The side force and drag is probably over-estimated due to the mesh being too chunky due to the mesh increasing rapidly at the side of the car.* If anything figures 5.2 to 5.4 show the car is more yaw sensitive than anything else, there is little avoiding this due to the 27 degree seating rule. It is stable for low angles of yaw in lift, and in the most likely operational speed range of 20-30 m/sec. For the design dive angle of -1.5 the car is stable for the speed range to 200km/h.

5.2.2 Surface Pathlines

Previous chapters plotted pressure coefficients and turbulence on the surface as an improvement in a shape was required. As we are studying the performance of the shape itself at different operating conditions it is a little more insightful to plot the surface pathlines. Essentially this is where the fluid closest to the surface is travelling, and if oil visualisation tests were ever to be carried out they would hopefully show similar patterns.

The top plan view pathlines are shown in figure 5.5, where it is easy to see the flow over the array surface and the disturbance around the canopy. At higher angles of yaw this canopy disturbance increases due to the vorticity in the radius between the canopy and the array increasing in strength. The separation and vortex roll up is noticeable from 10 degrees yaw on the leeward side (opposite the cross flow direction) of the canopy. The rear side rail taper seems reasonable from the pathline deviation for no yaw angle appears to be a natural direction the flow is moving, the front

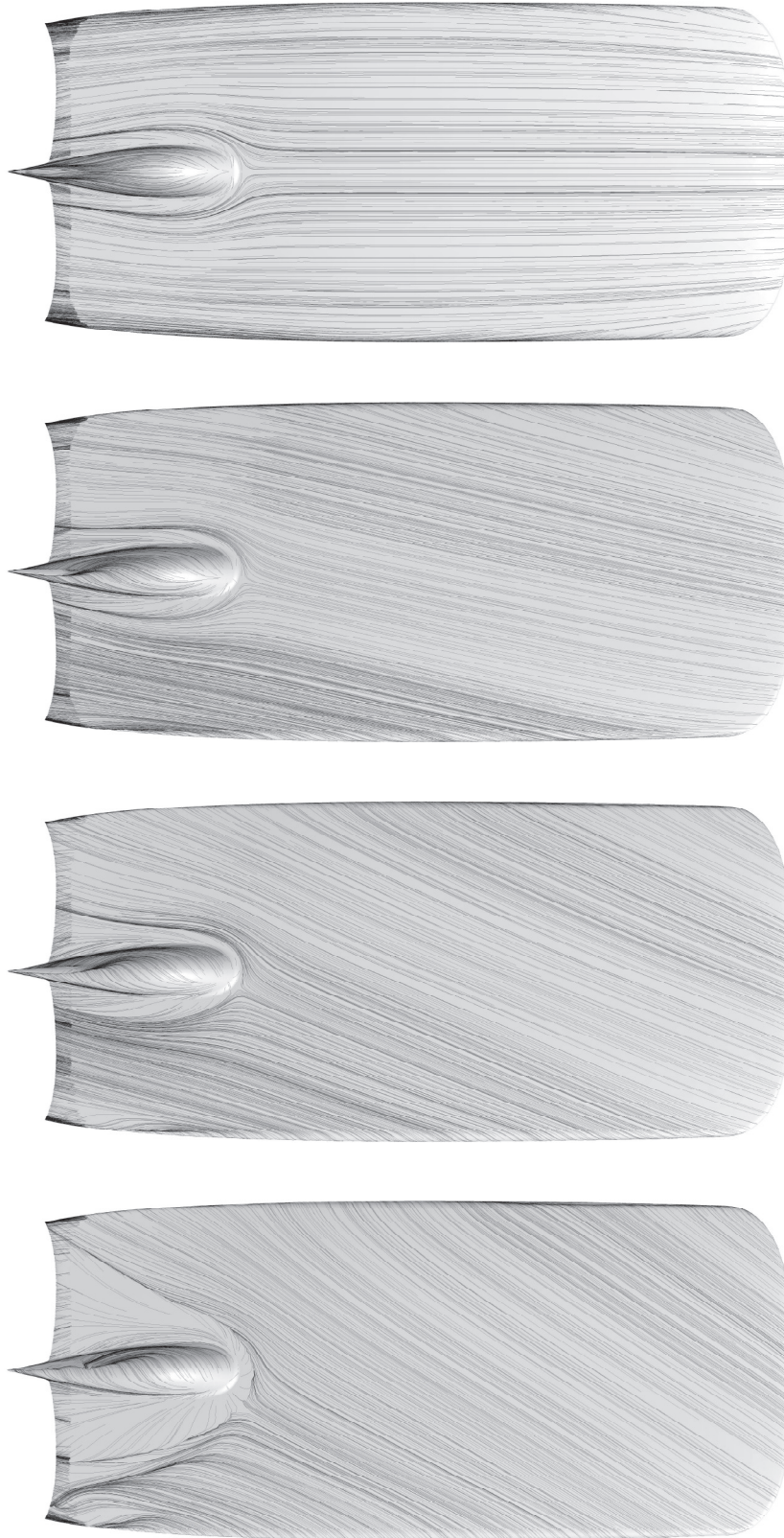


Figure 5.5 Surface Pathlines Top View

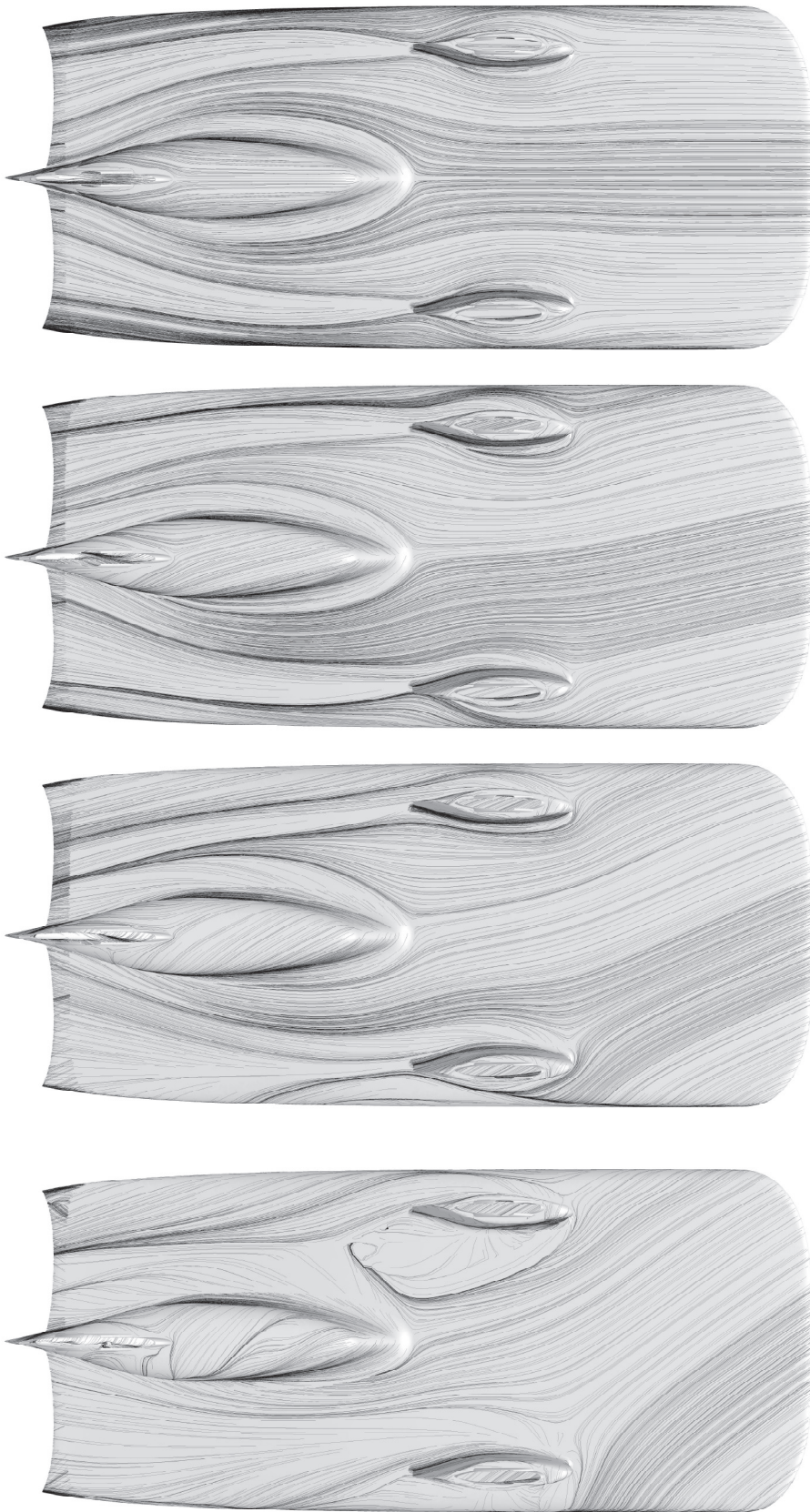


Figure 5.6 Surface Pathlines Bottom View

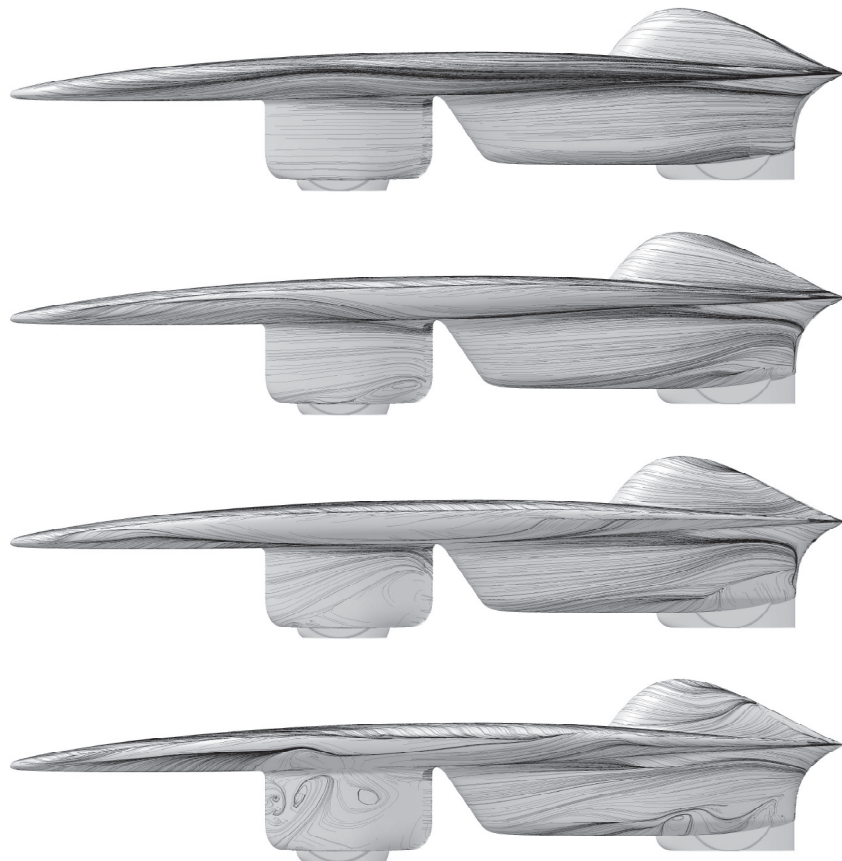


Figure 5.7 Surface Pathlines Leeward Side View

corners could have been profiled a bit further back however the maximum area was still required for the array and the slight drag increase was most likely outweighed by the array power increase.

The underside surface pathlines in figure 5.5 indicate how complex the flow is beneath the car and where most of the drag is likely to come from. When the car has no yaw the vortices forming from where the bumpod and the wheel fairings meet the bottom surface dominate. The amount of air the bumpod pushes out and inturn sucks back in from its widest point causes a significant deviation of the wake coming from the wheel fairings. A better profiled wheel fairing and fillet radius may help to reduce this. As the yaw angle increases the windward wheel fairing shields the bumpod and inturn has less disturbance in the wake compared to the leeward fairing which has a large wake and at 20 degrees appears to move out and up onto the upper surface. At the highest angle of 30 degrees the flow is highly unstable and the windward wheel fairing looks to have stalled completely. The fillet vortex on the bumpods windward side now appears to join with the wake of the leading wheel fairing too. Interestingly

the leeward wheel fairing seems to act as a turning vane for the leeward side of the bumpod, ensuring the oncoming flow is 'deflected' into the wake of the bumpod on that side and effectively tidying up the flow there.

Figure 5.7 shows the pathlines on the leeward side of the car. At 0 degrees yaw the wheel fairing slightly pushes the flow out on the side rail of the car, but for the most part it appears to be good, clean attached flow. As the yaw angle increases the lines tend to bunch up on the top and bottom most parts of the side rails with few lines apparent on the side rails themselves, this is due to the vortex starting to 'roll-up' off the top of the car. Also clear from 10 degrees onward is a messy swirling pattern near the front and rear wheels. This is likely because of the wheel and ground interaction forming a large vortex in the narrow gap. It may appear strange blocks are in front and behind the tyres. These 'boots' are to assist the solution as the gap between a cylinder and a flat surface gets infinitely small and highly skewed. These boots help limit the gap and if they were to be used on the actual car would assist in reducing the drag as the interaction between the spinning wheels and the fluid is highly draggy.

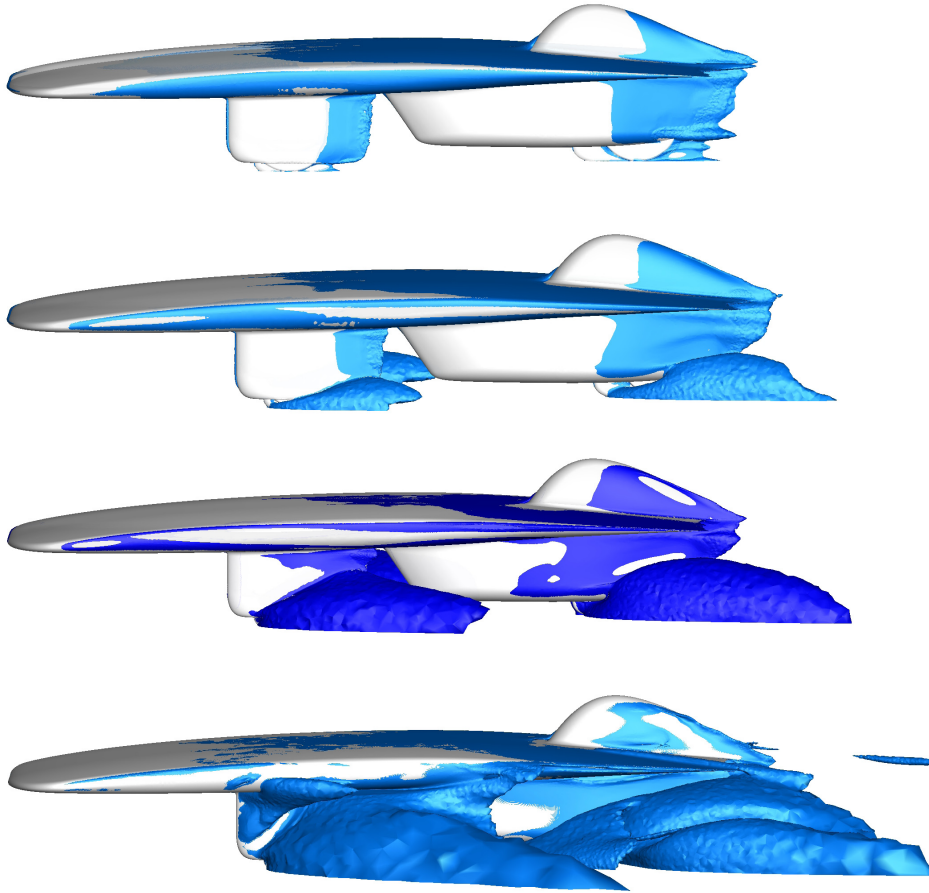
5.2.3 Wake Velocity

The off surface flow structure shown in figure 5.8 is an iso-surface of velocity. This is essentially each point in the mesh at which a given quantity is the same, in this instance 15 m/sec or 50% of the freestream velocity, and a surface is then made of these points all stitched together. It is useful as it shows where the fluid structures indicated in the surface pathlines of figure 5.5, 5.6 and 5.7 move to in the actual flow.

For no yaw there is very little low speed flow that extends a significant distance from the rear of the car, indicating the flow quality is quite good. There is however a little 'bubble' of air sitting on the back of the bumpod and the wheel fairings. It is not too bad, however a slight reprofile of the rear taper and extending the length a little bit may alleviate this, but its not of great concern as the flow is not fully separated.

As yaw increases there tends to be less low velocity on the windward side and more low velocity on the leeward side, which is obvious as the flow is moving across the car more. From 20 to 30 degrees yaw the leeward side of the canopy shows a quite random velocity distribution due to the vortex formed by the canopy. The flow structures that dominate are the wheel/ground interactions, these are shown to exist in the surface pathlines however the size and strength is evident here.

a)



b)

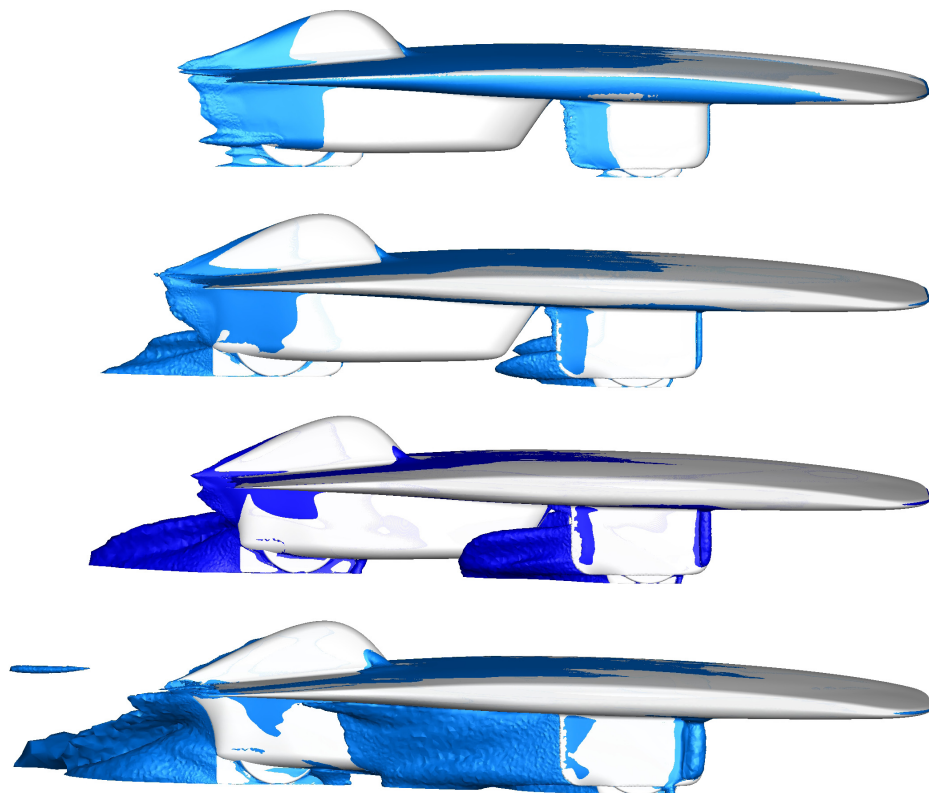


Figure 5.8 a) leeward side b) windward side Iso-Surface 15m/sec

5.2.4 Wake Vorticity

The vorticity iso-surfaces in figure 5.9 to 5.13 show where and if a vortex actually forms given the previous information of the surface pathlines and the wake. Figure 5.9 shows a transparent iso-surface with the pressure coefficient on the surface underneath. This shows the link of the C_p rise at the back of the car (if it is too quick) and the instability of the surrounding flow. It is clear that as the C_p is consistently low (green) that when it jumps to a higher (yellow) level there is an increased level of work on the fluid by the shape. It cant handle this and becomes a little dirty or unstable. The front wheel fairing appears to create almost as much dirty flow as the bumpod. For the most part it follows the car quite nicely and even remains attached to the car quite well over the upper surface, only becoming unstable at the end.



Figure 5.9 Vorticity Iso-Surface and Surface Pressure Coefficient Plot

Getting a more detailed picture of the overall car and the influence yaw has on the flow structure we move to figures 5.10, 5.11 and 5.12. At 0 yaw the vorticity sheets of the rear wing as normal, however the tip vorticity is no stronger than the bumpod, indeed there is no defined vortex 'tube' coming of the wing tip or side rail at all, showing that the intended effect of the side rail and Bat-wing is working quite well at 0 yaw. As the yaw angle increases it is clear that a vortex does form from the front corner on the leeward side and sticks to the side rail until at 30 degrees when the flow is entirely unstable and actually merges with the wheel fairing. The canopy produces a very small vortex towards the rear at 10 degrees, perhaps smaller than first thought by the surface pathlines, however at 20 degrees it increases in strength. At 30 degrees an additional vortex forms at the windward side wing tip. From 20 degrees an additional vortex is formed mid-way down the side rail, this is due to the inside vortex from the leeward wheel fairing spilling out and over the side rail. The size and strength of the vortices forming from the wheel/ground interaction again are quite large and a significant feature of the flow field when the car is in yaw.

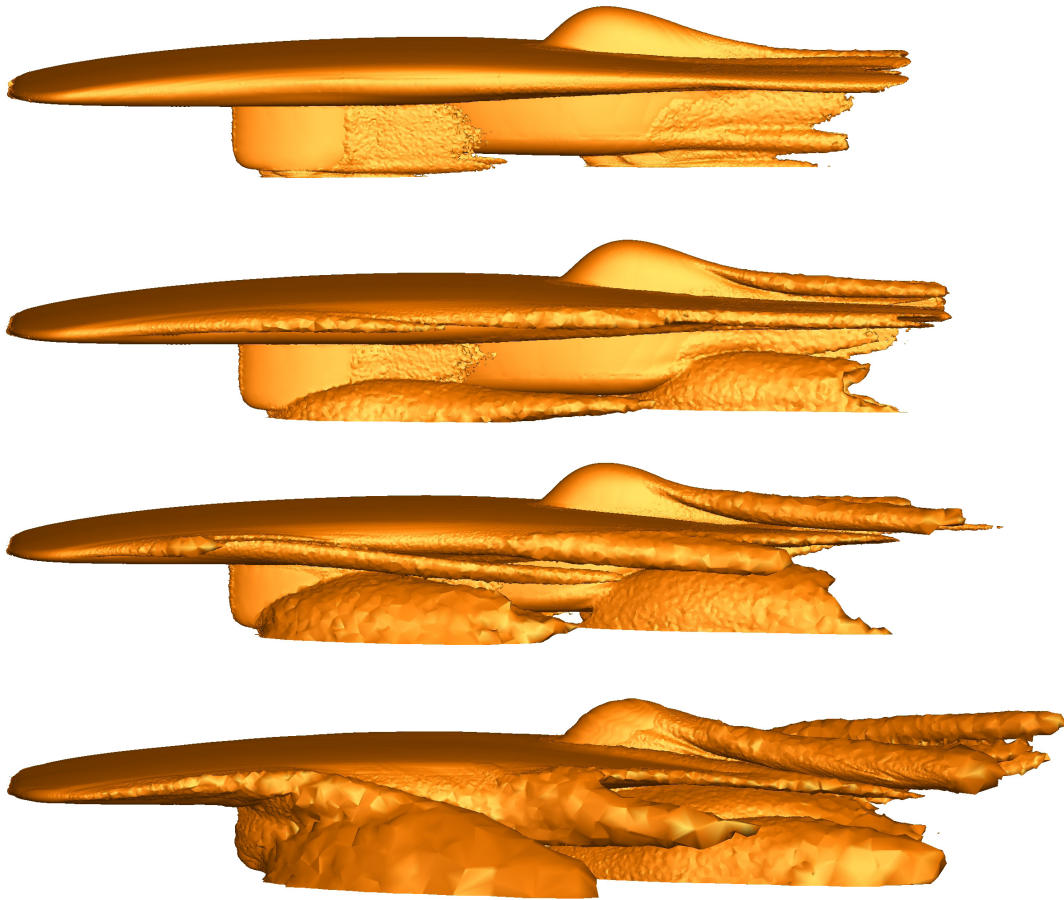


Figure 5.10 Off Surface Vorticity Iso-Surface, Side View

However the plan view of the vorticity reiterates a few points relating to the side rail and Bat-Wing wake 'sheet' coming off the car, in figure 5.11 its dominated by the vorticity off the canopy. It does indicate the tip vortex is not that strong, significant when you consider how big the wing is and the speed it is travelling. As the car yaws the deviation of the vortex on the canopy increases and from 20 degrees to 30 degrees the flow underneath the car spills out and up over the leeward side rail.

Figure 5.12 shows the vorticity under the car the significance of the windward side wheel fairings interaction with the bumpod is clearly defined here, as is where the additional side rail vortex is coming from the interaction of the junction of the wheel fairing and the underside of the car. Although the ground vortex is in the way as it is bigger it is clear it is coming from the inside, particularly as we move to figure 5.13 to take an angled view under the car. Which shows the windward side wing tip vortex increase. Crucially there is no vortex roll up from the side rail of the windward side of the car at all, ensuring good flow across the top of the car at all times.

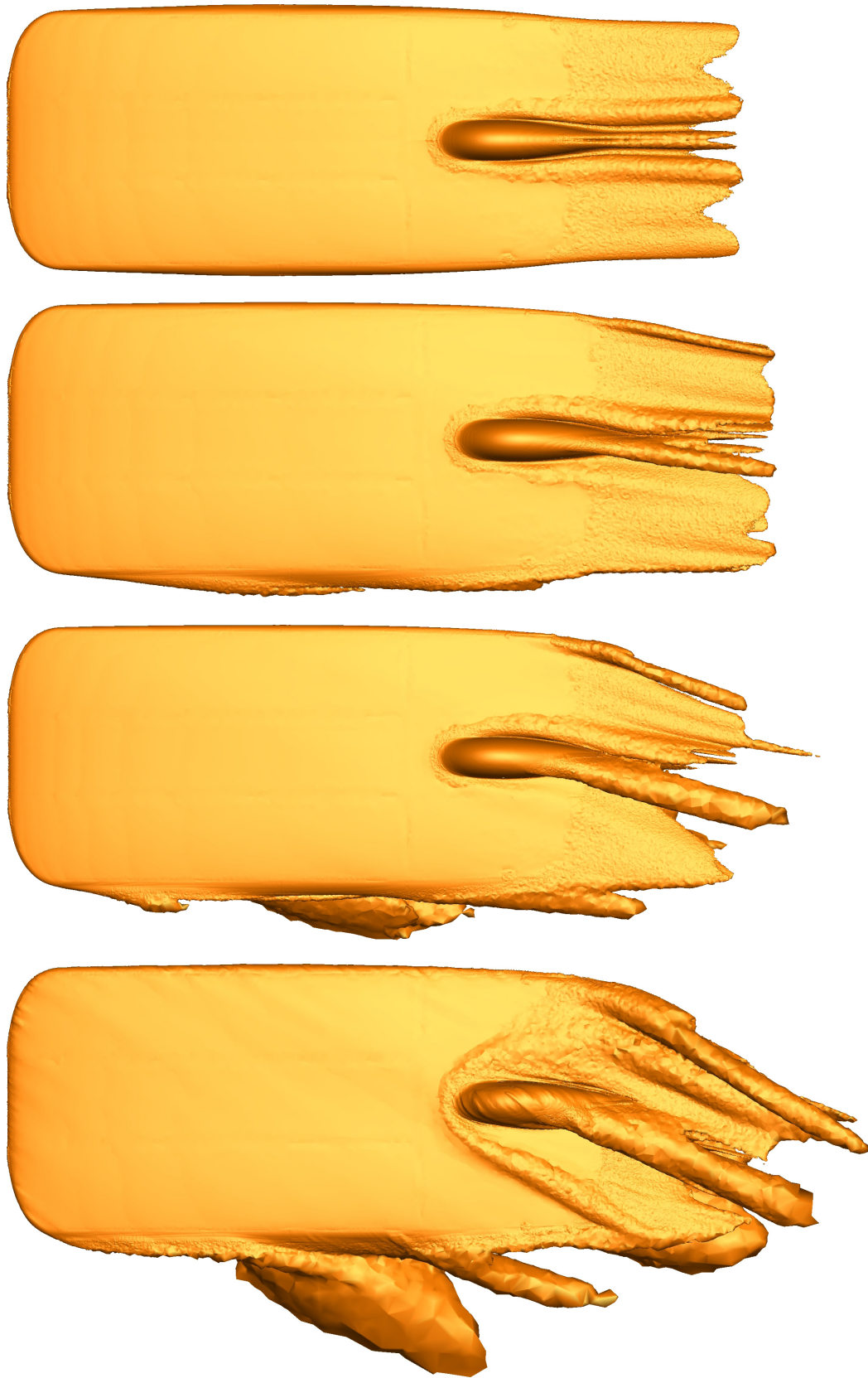


Figure 5.11 Off Surface Vorticity Iso-Surface, Top View



Figure 5.12 Off Surface Vorticity Iso-Surface, Bottom View

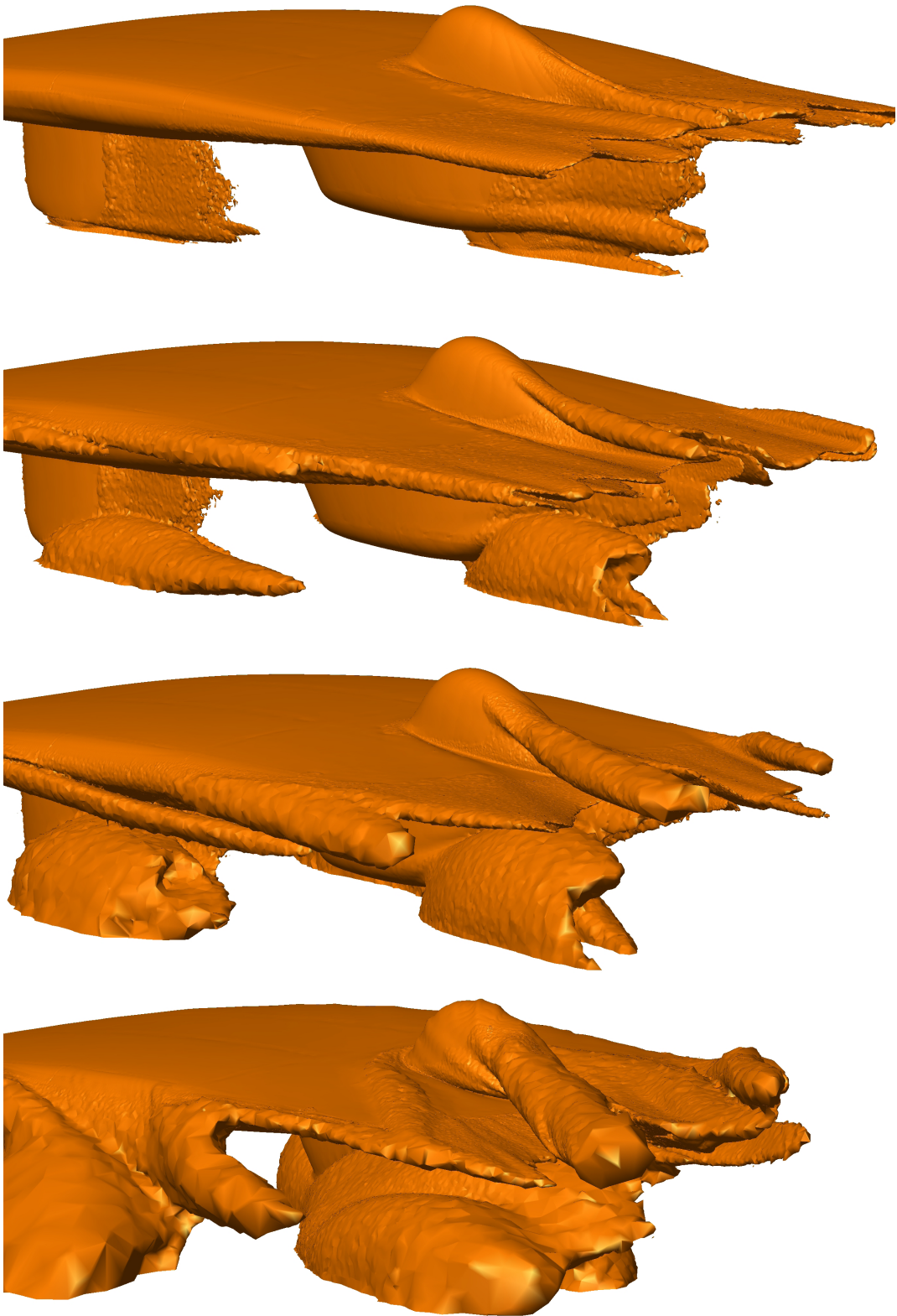


Figure 5.13 Off Surface Vorticity Iso-Surface, Rear Isometric View

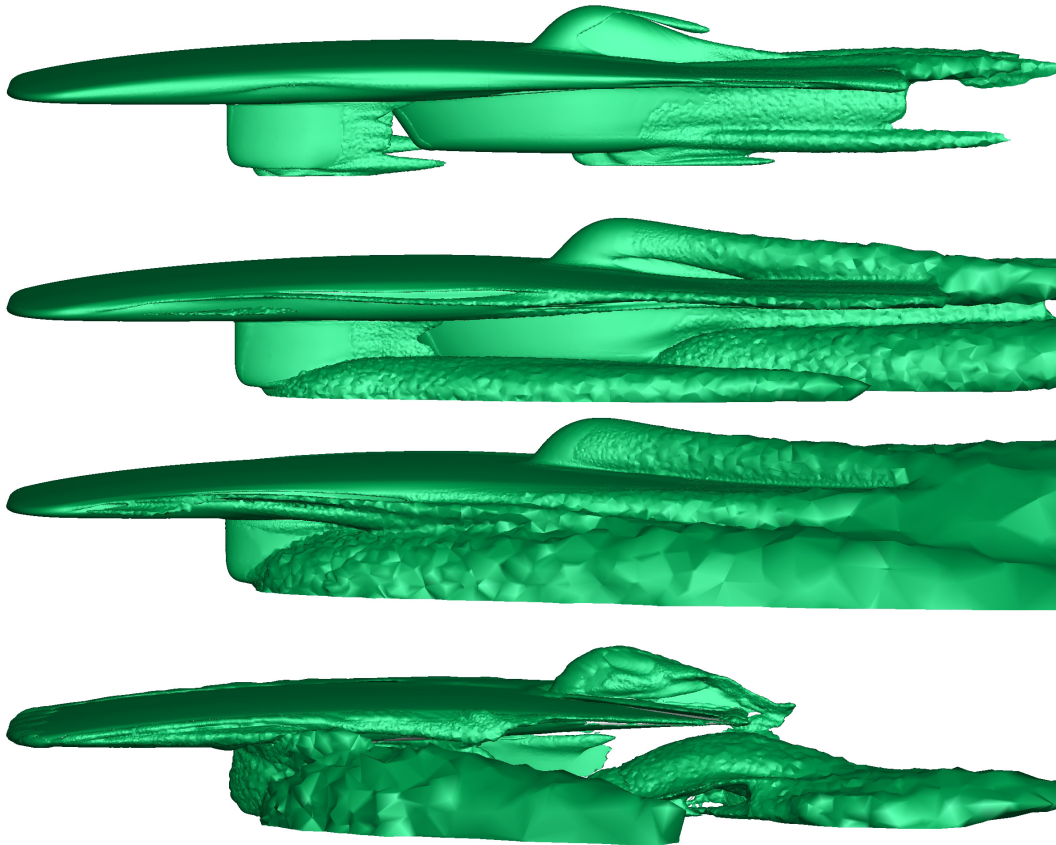


Figure 5.14 Off Surface Turbulence Iso-Surface, Side View

5.2.5 Wake Turbulence

Previous Iso-Surfaces indicated the velocity deficit and vorticity or flow rotation. Figures 5.14, 5.15 5.16 and 5.17 plot the turbulence in the flow, so where any instability is being made. It will correspond largely to where the big complicated separated flow structures are that have vorticity and turbulence, however there are some fluctuations that arise which are not due to vorticity.

The side view of figure 5.14 shows that the turbulence of the trailing tip of the car and the rear wheel/bumpod junction act very strongly. The former is the case due to it forcing the flow to remain on the car the longest thus channeling the most instability to that point, the later due to the spinning wheel and the bumpod/grounf inteaction being very unstable. The sheet coming of the trailing edge of the main wing itself is not that strong, which is indicative of not only the Bat-Wing but the benefit of a sharp trailing edge. There is a small increase in turbulence above the canopy at 0 yaw that slightly trails behind it, perhaps the curvature is on the limit of being too extreme.

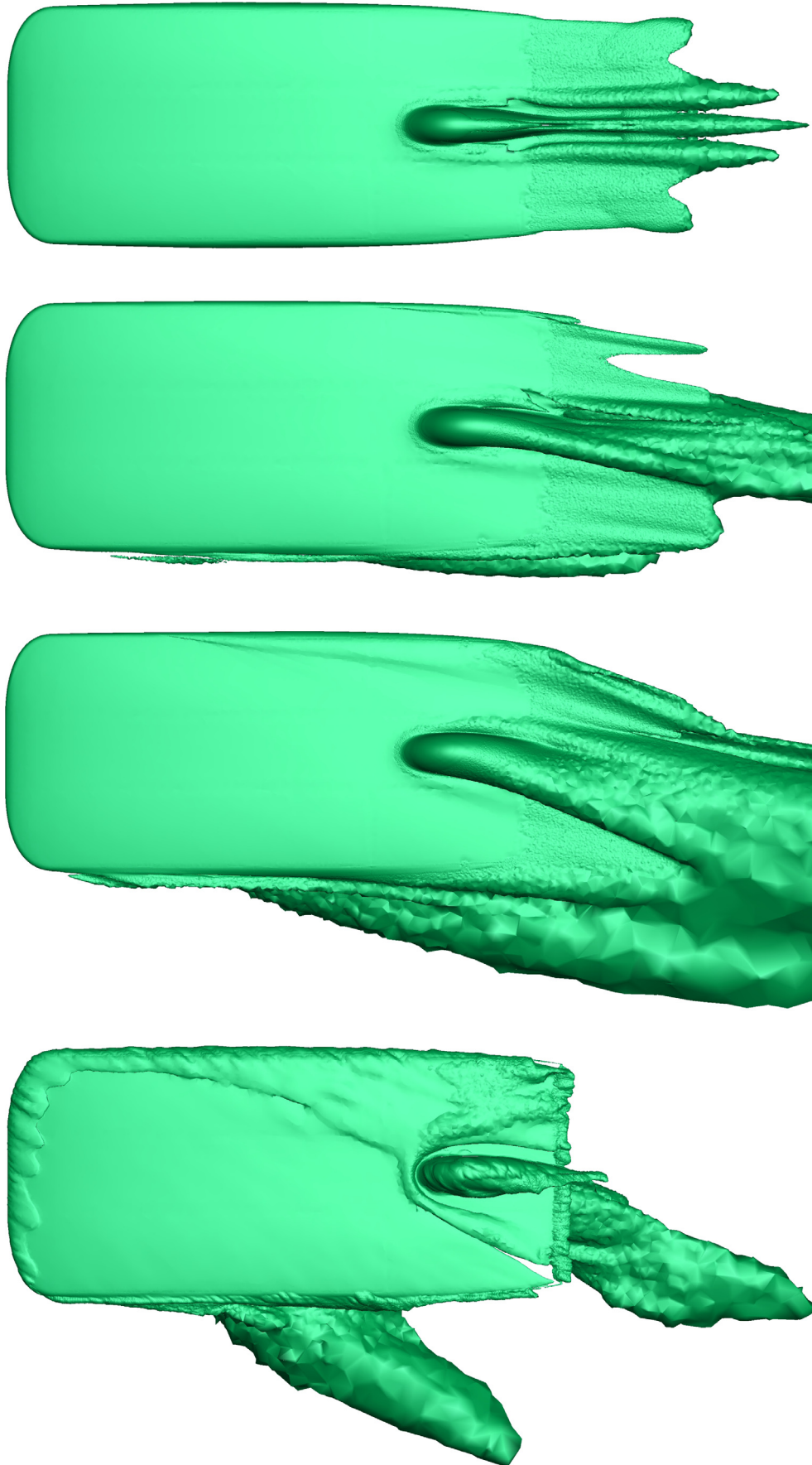


Figure 5.15 Off Surface Turbulence Iso-Surface, Top View

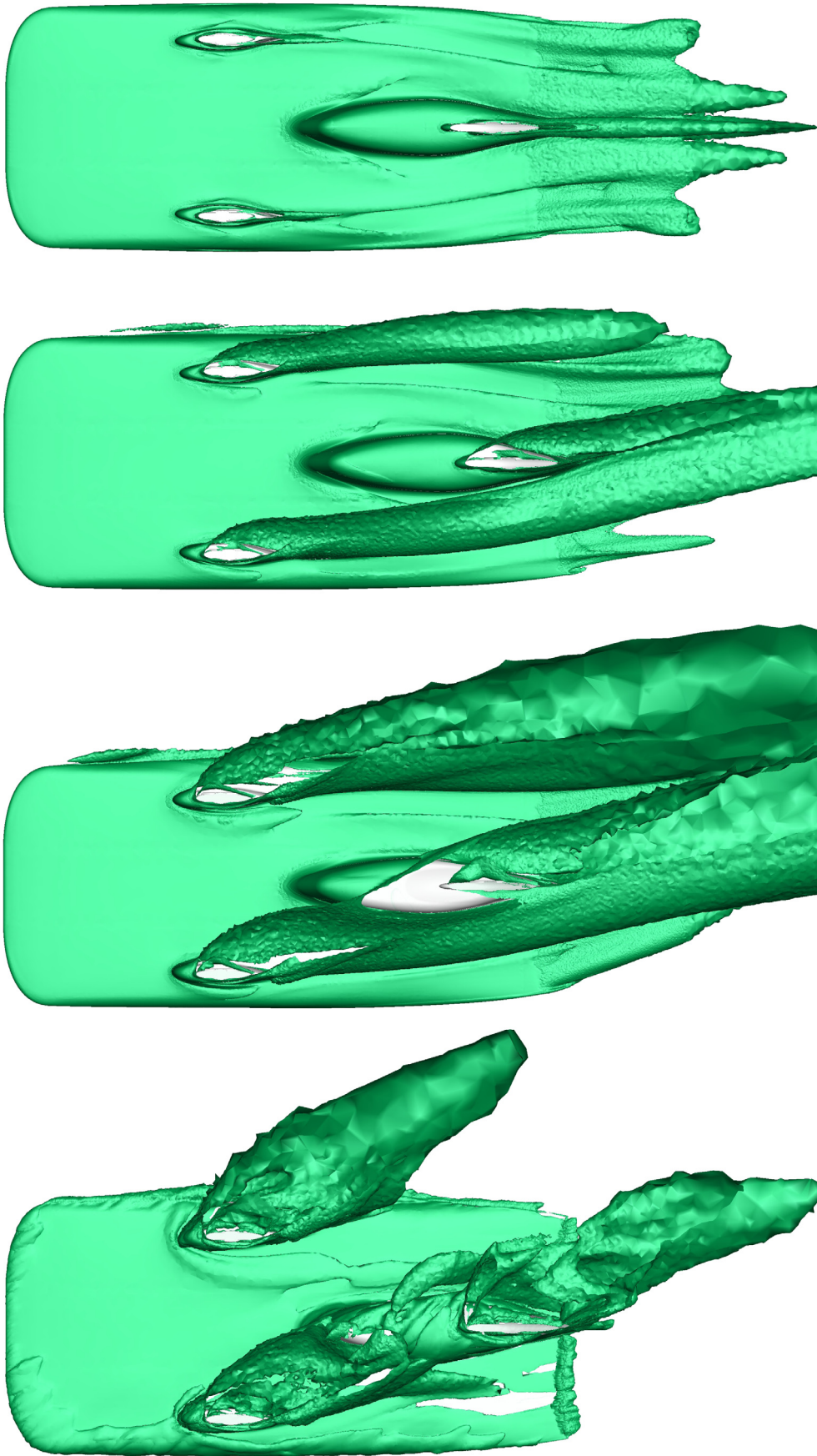


Figure 5.16 Off Surface Turbulence Iso-Surface, Bottom View

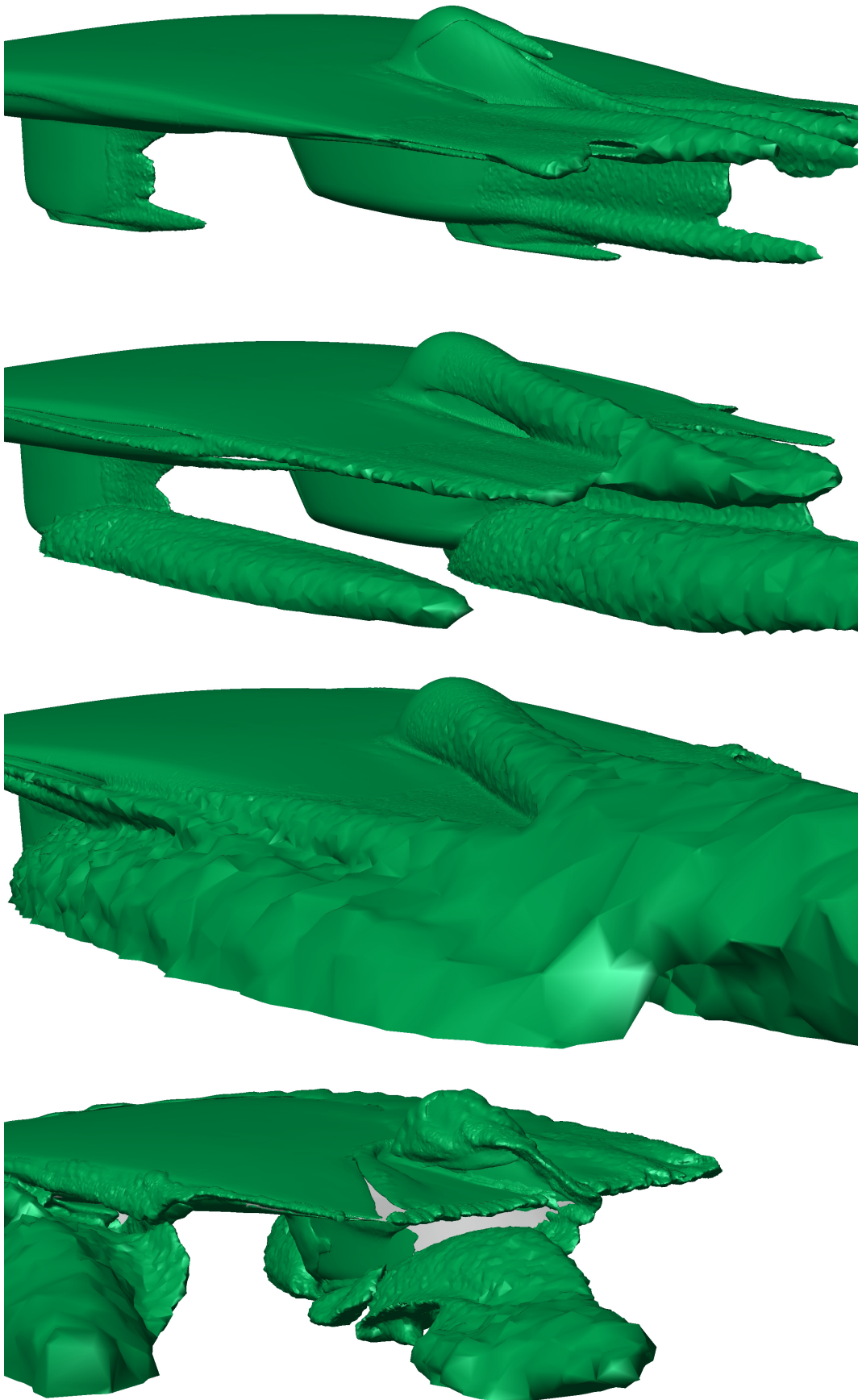


Figure 5.17 Off Surface Turbulence Iso-Surface, Rear Isometric View

The familiar trend of the increased yaw deflecting the turbulent wake behind the bumpod and the wheel fairings is maintained through figures 5.15, 16 and 17. As is a clearer indication of the turbulence of the interaction of the wheel and ground even with the 'boots' assisting the flow in this region. Perhaps on yaw the boots are detrimental to the flow itself, however the force report stated only takes into account the aerodynamic surfaces of the car, so to some extent this is negated. What is clear is the higher instability at increased yaw. Interestingly although the wingtip vortex forms on the windward side at higher yaw, the turbulence of this vorticity is small compared to the others given the turbulence level plotted does not indicate it is present at this level.

5.3 Conclusion

Having shown that the lift and drag coefficients are sufficiently small given the -1.5 dive angle of the main wing section it is deemed that not only will IVy be safe for the driver for the designed operating speed range it will perform quite well. Whilst being a bit yaw sensitive in certain conditions over 10 degrees, overall the flow quality over the car is of no major concern. The Bat-Wing concept and bumpod/canopy layout seems to have worked based off the iso-surface outlined above, and will only be properly evaluated by the stability and handling of the car in real life. There is room for additional refinement which is more appropriately conducted by thorough testing of the car (based off the data here) rather than commencing a new CFD program.

Performance

6

6.1 Introduction

Having built the car just in time for the event with testing limited to a basic mechanical systems check, the only real performance analysis of the aerodynamic design occurred during the race. The car winning silicon class and coming fourth overall in the challenge class was no feat of luck, the car had pace from the few set backs in the first day. However the ultimate proof of the aerodynamic design relative to the other more established and well funded teams such as Nuna, MIT and Michigan did not occur until day 4 and 5 of running. The overall average speed of the car through the event quoted as 76.3 km/h, Michigan 90.5 km/h and Nuna 91.9 km/h, but monitoring the individual times for the control stops showed the relative pace between cars over the same stretch of road for the same conditions.

Table 6.1 Day 4 Stage Split Times

(*-denotes they finished there 16:43 previous day)

Position	Team	A (km)	B (km)	time (min)	Av. speed (km/h)
1	Tokai	1766	2180	242	102.64
2	Nuna	1766	2180	293	84.78
3	Michigan	1766	2180	285	87.16
4	MIT	1494*	1766	348	71.38
5	SUNSWIFT	1494	1766	317	78.36
6	Principia	1494	1766	354	70.17
7	Aurora	1494	1766	340	73.06

Table 6.2 Day 5 Stage Split Times with 20 km/h gust cross wind

Position	Team	A (km)	B (km)	time (min)	Av. speed (km/h)
1	Tokai	2432	2719	194	88.76
2	Nuna	2432	2719	210	83.59
3	Michigan	2432	2719	206	82
4	SUNSWIFT	2432	2998	420	80.86

That direct comparison in the gusty conditions of Day 5 over the same stretch of road given that both Nuna, Michigan and Tokai had higher power Gallium Arsenide Solar Arrays is impressive, not least that the Silicon Array on IVy was slightly damaged when leaving Darwin. This is perhaps the best indication that the planned low drag and stability aspects of IVy were in fact realised in real world conditions that are impossibly difficult to replicate experimentally or numerically given the additional cross winds. Analysis of data post race by David Snowden shows a drag calculation based from wheel motor power (but not accounting for the slope of the road) of $C_D A_{(real)}=0.07$ or $C_{D,(real)}=0.11$, compared to table 5.1 given speeds were higher than 70km/h and the pitch of the car was altered slightly from the designed dive angle of -1.5 this comparison to the CFD result especially for drag is good.

It shows that the pace of the car evolved the more that it ran, and that should it have been finished earlier the car would have started the race as fast if not faster than it finished. Given the lack of driver confidence is reflected in the early speed, more testing time would also have boosted this crucial area too. Therefore future development and testing of this car (considering this was the first time it ran properly) will ensure a faster car in future events. Ultimately the “luck” was that the car finished were it rightfully should have rather than lucked into speed as it was legitimately faster than the cars around it and that it ended up beating.

5.2 Improvements

Several ideas were considered for the initial design of the car, however due to time restraints and the need to get the basic format of the car finished these ideas were dropped. These will be addressed for consideration and hopefully further use on the car to develop it. Areas of the car and the subsequent proportion they contribute to the overall lift and drag are outlined in table 6.3. The majority of the drag is generated by the viscous effects of the main wing section of the car, where as the majority of the downforce comes from the ground effect interaction of the bumpod. Importantly table 6.3 indicates where the most drag improvements are to be made, namely the main wing section of the car, the wheel fairings and to a lesser extent the bumpod.

Improvements that can be made to the main wing section of the car to reduce drag involve considerations that the CFD can't account for given they relate to

Table 6.3 Lift and Drag Composition

(*-denotes lifting where as other components generate downforce)

Part of Car	% of total C_D	% of total C_L
Canopy	0.6	-14.6*
Bumpod	2	59.5
Main Wing Section	83.4	35.8
Wheel Fairings	14	19.3

manufacturing techniques. The first given the paint job is the surface finish of the car, the viscous drag component is high thus making sure the surface of the car is highly polished and free of dirt is highly important. Particularly the underside of the car due to its surface area is in ground effect, as surface roughness will cause the viscous drag to increase significantly. The next relates to how the car was put together, the tape running around the edge and leading edge of the car will cause the flow to be 'tripped' earlier and will also increase drag. A more aerodynamically efficient solution would be to cut the leading edge and side rails off the top array surface and bond them to the lower part of the car, similar to Tokai's solution, thus having some handle access to lift the array of the car. This will ensure the flow remains less turbulent over the car, its possible along the side rail that the tape may cause a vortex to roll up over its length at 0 yaw. The weight penalty should not be too detrimental given the vastly quicker access and increased aesthetics of the car. Additionally the surface roughness of the top surface due to the array will not help the drag either, taping up the gaps between solar cells will also limit the amount of instability and turbulence to the flow as these tiny gaps can produce unstable vortices bursting out of them.

The next area of improvement is the wheel fairings, ideally these should be remade as the shape causes too much trailing edge turbulence and drag (see figure 5.9). Ideally this would be made with some slight camber (curvature i.e. not symmetric) so that some 'sail' can be generated and they can continue to effectively act as flow

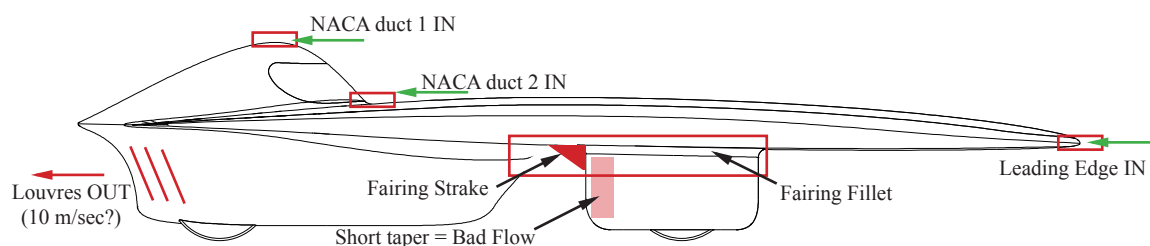


Figure 6.1 IVy performance additions

turning vanes for the bumpod. Also the wheel fairing's fillet to the underside needs to be optimised, it should be made slightly bigger to reduce the amount of vorticity and turbulence it generates which can be seen to run down the length of the underside of the main wing in chapter 5; this will also be reduced with a new fairing profile. Additionally a rear strake (or an incorporated extension of the new fillet fairing at the rear) will help breakdown any vorticity produced by the interaction of the rear of the fairing and the underside of the wing, the strake is noted in figure 6.1.

Successful employment of ducting for cooling should be able to actually reduce drag if done properly. Introducing a NACA duct on top of the canopy should spoil some of the lift and lower the induced lift component. A proper NACA duct just above the radius at the front of the canopy (where a simple hole currently is) will do a similar thing; do one or the other not both. Ducting flow through the internals from the leading edge of the car can limit the high pressure build up due to the stagnation point at the front of the car (reducing pressure/form drag).

Making sure the ducted air comes out of the car efficiently is important, it is for this reason that the rear ducting louvres shown in the original concept sketch of figure 1.1. The 'blown trailing edge' is to recover the lower speed flow in the area seen by the 15 m/sec bubble at the rear of the car in figure 5.8. By returning air that is tangential to the surface at a faster velocity than the adjacent flow the 'dirty air' that was there previously will be minimized. This requires careful ducting leading up to the exit louvres and some mesh or packed tubes to straighten the flow and lower the turbulence (like a wind tunnel which is seen in the UNSW Aerodynamics lab). To force the flow out a fan would be required to dump the air out the back and ensure it does not leak back in the rear section of the car.

Further testing of the car will highlight additional performance gains. If the trailing edge flow quality of the fairings and the bumpod can be established and have sufficient correlation to the CFD data presented here, then it is possible to recover the flow with the proper use of vortex generators. Shown in figure 6.2, a simple vortex generator produces two counter rotating vortices that mix the flow. They essentially refresh the fluid close to the surface which has been over worked by the extreme curvature of pressure demands with flow that is further away from the surface. They cannot be too large or will themselves increase drag, a 3mm height limit would be sufficient located very close to slightly ahead of the bad or 'dead' flow.

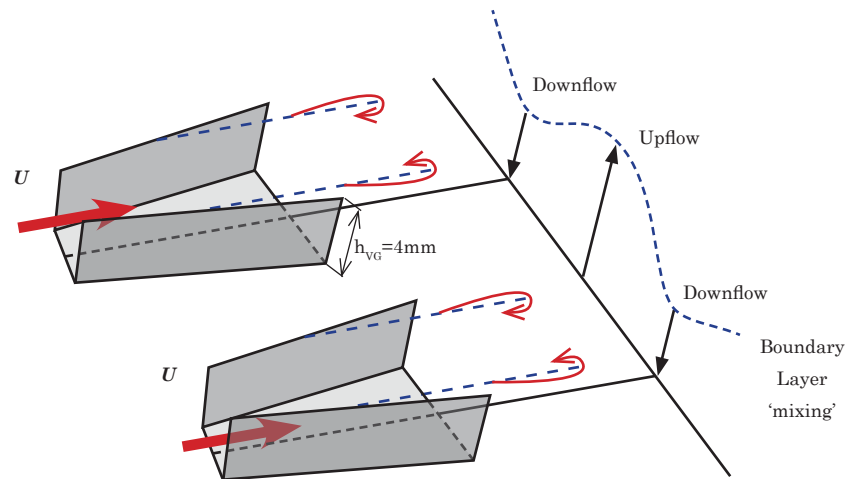


Figure 6.2 Trapezoidal Type Vortex Generators

6.3 Testing

The simplest form of drag testing is find a flat bit of road and stable weather conditions and let the car decelerate from its own rolling resistance and the aerodynamic drag. The former should stay constant with given weight and tyre pressure, the later should change only with improvements to the aerodynamics as outlined previously. The longer the distance the car takes to decelerate for a given speed differential then the lower the aerodynamic drag should be. There are other important methods of testing relating to the flow field around the car in order to validate the CFD .

On Surface flow: using dye or highly viscous oil to cover the surface of the car in a few locations that are of interest to generate the kinds of pictures shown in figure 5.5, 5.6 and 5.7. If the flow good quality it will follow the shape well, if there is turbulence or messy flow it will bunch up and make strange (if not pretty) patterns.

Off Surface: Using clearly visible tufts (small pieces of a relatively thin string a few inches length of good contrast to the white car) will indicate where the flow is moving. It is similar to oil/dye surface testing but shows how unstable the flow is by the degree of flapping/moving the tufts do. Additionally placed on corners of the wing tips and the trailing edge of the fairings and main wing it will show any vortices as this will result in the tufts swirling. These could be a fraction longer than tufts placed directly onto the surface to get a little more information. It is important not to cover the whole car in them, use them sparingly so they don't interfere with each other. Placing them in internal fillets is also a good idea.

Equipment: 3 digital weather stations from Jaycar (\$180 each) at start/middle/end of test run to get wind speed and direction. Mixture of Kerosene and food dye or UV

sensitive dye (and a UV light) for oil surface flow visualisation. If Kerosene is too abrasive something like WD40 could be an option. China clay method can be used but it would be messy. It is important to look at the oil surface visualisation as soon as possible, as if the Kerosene hasn't evaporated then it will start to run.

6.4 Towards Sunswift 5.....from IVy to Eve?

It is impossible to build one car without thinking about the next and what would be done differently. Several ideas that were thought which could be considered for future evolutions of the car are:

Optimising the core on the bottom surface of the main wing to where it is needed so that is not covering the entire bottom shell will reduce the weight. Having the shell stiff enough to cope with aerodynamic forces is appropriate to limit deflections and the increase to drag that may result. However having the bottom shell stiffer than the chassis/monocoque is not ideal.

Utilising a 'rear wheel steer' system will have the benefit of being able to lock the front fairings and drag optimise them entirely. If the wheel fairings are designed with proper camber by locking them the flow will remain consistent over the bumpod. It will require a mechanical steering system set up so that the driver does not have to steer left to turn right, and the front wheels can have a simple vertical shock. By doing this it would be possible to make the main wing section exceptionally thinner as currently it is limited to the wishbone and suspension travel. There is plenty of room in the bumpod to design a mechanical system to do this. The critical issue being the rear steer wheel still has to compress with suspension movement, yet the steering wheel and steering column must remain stationary.



Figure 6.5 Renault F1 Aerodynamic Mass Damper

The Renault Formula One team had a clever trick up their sleeve in 2006, they employed the use of an “aerodynamic mass damper” on their car. This countered the pitch sensitivity of their car and helped the aerodynamics by having a spring/mass/damper configuration which moved counter to the pitch of the car. By assisting the car to remain in the set up configuration in a solar car application which are pitch sensitive due to the plan area, lack of camber and drag optimised nature of the main wing this will help stabilise the car and keep it in a low drag configuration.

The trade off for downforce and drag versus grip is a worthy investigation, particularly for racecar performance on a closed circuit race track. Generating additional downforce for increased cornering grip/speed which on the straight road during the race to Adelaide is not important may have benefit in qualifying or in future racetrack based competitions. Utilising downforce that is possible for little drag penalty due to ground effect of these cars by a Gurney flap on the trailing edge, a little more static dive angle of the car or additional winglets and or wings could generate additional performance. A connecting wing low to the ground could also connect the two ‘locked’ front wheel fairings.

Moving to Aerofoil ‘spoked’ wheels in a tri layout will reduce the viscous drag of the wheel spinning inside the wheel fairing (which is closed). This has been done in other forms of competition like olympic velodrome race cycles and recumbent faired bicycles (youtube it). As these are fully enclosed bikes and they found spoked wheels reduced the drag and power needed to get them going. The gaps in the wheel may also reduce the messy flow in yaw at the wheel contact patch.

Many thanks to the Aero CFD team, and on behalf of Graham Doig and myself thanks to Clara Mazzone for giving us more or less free reign of the design and letting us give birth to IVy.

Contact details for any questions

Christopher Beves

cbeves@hotmail.com

Graham Doig

grahamdoig@hotmail.com

Make the subject heading Sunswift IVy or something so we don't miss it.